This manuscript is a preprint and has not been peer reviewed. The copyright holder has made the manuscript available under a Creative Commons Attribution 4.0 International (CC BY) license and consented to have it forwarded to EarthArXiv for public posting.

Compound drought and heat exposure and lean-season food insecurity in Zimbabwe: agro-ecological heterogeneity in a 2009-2025 district panel

Authors. Handsome Bongani Nyoni[1]*, Lesley Chawira[2], Perez Livias Moyo[3], Zororo Chinwadzimba[4], Rutendo Sibanda[4], Mashford Zenda[5] ,Happy Mathew Tirivangasi[6]

[1] Place Alert Labs, Department of Surveying and Geomatics, Faculty of the Built Environment, Midlands State University, Gweru, Zimbabwe

[2] Department of Surveying and Geomatics, Faculty of the Built Environment, Midlands State University, Gweru, Zimbabwe

[3] Climate Environment and Health Department, Centre for Sexual Health and HIV AIDS Research (CeSHHAR), Harare, Zimbabwe

[4] Department of Environmental Health, Faculty of Environmental Science, National University of Science and Technology, Bulawayo, Zimbabwe

[5]Department of Sustainable Food Systems and Development, Faculty of Natural and Agricultural Sciences, University of the Free State, Republic of South Africa

[6] Department of Social Sciences and Philosophy, University of Jyväskylä, P.O. Box 35, FI-40014 Jyväskylä, Finland

* Corresponding author: nyonih@staff.msu.ac.zw

This manuscript is a preprint and has not been peer reviewed. The copyright holder has made the manuscript available under a Creative Commons Attribution 4.0 International (CC BY) license and consented to have it forwarded to EarthArXiv for public posting.

Abstract

Food security early warning in sub-Saharan Africa relies entirely on rainfall, although co-occurring hazards can produce impacts larger than the sum of their separate effects. Researchers have rarely applied compound-event framing to African food security outcomes, but harmonized sub-national data now make it testable.We test whether co-occurring growing-season moisture deficit and heat predict district-level food insecurity in Zimbabwe better than moisture deficit alone, using a panel of 84 district and urban-council units over 2009 to 2025 (1,342 district-seasons). Harmonized IPC-compatible phase classifications are combined with six-month SPEI and counts of days above each district's own 90th percentile of daily maximum temperature. Nested two-way fixed effects models are compared on within-sample fit and leave-one-season-out error, with clustered, Conley, and permutation inference. Pooled nationally, the compound interaction is small (β = +0.030, p = 0.083), not robust to spatial dependence (Conley $p \geq 0.105$; season-block permutation p = 0.35), and does not improve out-of-sample prediction. Within the driest third of districts, it is +0.116 ($p < 0.001$) and survives both checks (permutation p = 0.004). A pooled three-way model shows the driest third differs from the wettest (difference +0.051, p = 0.029), although the joint test across strata is weaker (p = 0.087). The compound mechanism is concentrated on the most marginal land.A single national compound-risk estimate would therefore understate risk where it is largest.Stratifying seasonal outlooks by agro-ecological zone costs little: ERA5-Land is operational and freely available, and the district-specific hot-day threshold is already a per-stratum calculation.

Keywords. compound events; food security; drought; heat; Zimbabwe; SPEI; IPC; fixed effects; early warning; agro-ecological heterogeneity

This manuscript is a preprint and has not been peer reviewed. The copyright holder has made the manuscript available under a Creative Commons Attribution 4.0 International (CC BY) license and consented to have it forwarded to EarthArXiv for public posting.

Plain Language Summary

Food security warnings for southern Africa rely almost entirely on rainfall: if the rains fail, a drought warning follows. But heat and drought often arrive together, and in other contexts (wildfires, floods, heatwaves) that combination causes more damage than either hazard alone. This has barely been tested for food security in Africa.We tested it directly for Zimbabwe, using 17 years of data (2009 to 2025) covering 84 districts. We combined official food-insecurity records with independently measured drought (a standard rainfall-and-evaporation index) and heat (the number of unusually hot days each growing season).Across the whole country, the drought-heat combination added very little beyond drought alone, and that small effect did not hold up under stricter statistical checks. But in the driest third of Zimbabwe's districts, it mattered a great deal: nearly four times larger, and it held up under every check we ran. A separate test confirmed these dry districts behave differently from the wettest ones.A single nationwide risk estimate hides exactly the places where the risk is real. The data needed to flag this (satellite rainfall and temperature records) are already free and already used operationally, so adding this check to existing early-warning systems would cost little. We also show, using standard future-climate projections, that this concentrated risk is expected to grow in the driest districts through the 2050s

1. Introduction

Zimbabwe's agricultural system is dominated by a single rainfed season running from October to April, and the country's food security is correspondingly dominated by what happens to rainfall in those months. Successive droughts, most severely in 1991/92, 2015/16, 2018/19 and 2023/24, have produced national maize deficits, emergency appeals and large movements in the share of the rural population classified in IPC Phase 3 or above. The monitoring systems that detect these events, from the national ZimLAC Rural Livelihoods Assessment to the regional FEWS NET outlooks, treat seasonal rainfall as the primary environmental driver. The

This manuscript is a preprint and has not been peer reviewed. The copyright holder has made the manuscript available under a Creative Commons Attribution 4.0 International (CC BY) license and consented to have it forwarded to EarthArXiv for public posting.

consequences fall most heavily on smallholder and communal-area households, whose limited access to finance, extension and institutional support constrains their ability to adapt to climate hazards that already cause crop and livestock losses (Zenda, 2024, 2026; Zenda et al., 2026). Diversified agroecological production provides an important local buffer against failed seasons (Rudolph & Zenda, 2025).

The case for widening that view is now strong on three separate grounds.First, the physical case. Evapotranspirative demand rises with temperature, so the same rainfall total supports less crop water availability in a hotter season. A rainfall-based index is blind to this by construction. Indices that incorporate atmospheric demand, most prominently the Standardized Precipitation-Evapotranspiration Index (Vicente-Serrano et al., 2010), capture it, but they are still univariate: they compress moisture and demand into one number and therefore cannot say whether heat does anything beyond its contribution to the water balance.

Second, the agronomic case. Maize, which supplies the majority of caloric intake in rural Zimbabwe, is sensitive to high temperature during flowering and grain fill through mechanisms that are not purely hydrological, including pollen viability loss and accelerated phenology that shortens the grain-filling period. These mechanisms imply that heat and moisture deficit should interact rather than simply add, and a meta-analysis of over 120 combined-stress experiments confirms the direction: drought and heat applied together cut yield substantially more than either stress alone, through the same shortened-cycle, reduced-harvest-index mechanism, with the reproductive stage most exposed (Cohen et al., 2021).

This manuscript is a preprint and has not been peer reviewed. The copyright holder has made the manuscript available under a Creative Commons Attribution 4.0 International (CC BY) license and consented to have it forwarded to EarthArXiv for public posting.

Third, the methodological case. The compound event literature (Zscheischler et al., 2018, 2020; AghaKouchak et al., 2020) has developed a clear framework for hazards that co-occur and has shown repeatedly that impacts from co-occurring hazards exceed what independent treatment of each hazard would predict. That framework has been applied extensively to fire, flood and heat mortality, and comparatively rarely to food security. In sub-Saharan Africa specifically, where the impact data has historically been too sparse and too inconsistently defined to support panel estimation, it has scarcely been applied at all. The closest methodological precedent is Schlenker and Lobell (2010), whose panel analysis of over 20,000 African maize trials found yields falling roughly 1 per cent per degree-day above 30°C under rainfed conditions and 1.7 per cent under drought: a nonlinear, fixed-effects treatment of heat that this paper's own district by season-year design follows directly, extended here from yield to the downstream food-security outcome and from an additive heat term to an explicit interaction.

That last constraint has recently eased. The harmonized sub-national food security dataset (HFID) reconciles IPC, Cadre Harmonisé, and FEWS NET classifications into a single monthly series on consistent sub-national units from 2009 onward, which for the first time makes a long, comparable panel of food security outcomes available for African countries. On the exposure side, CHIRPS version 3 and ERA5-Land provide daily rainfall and temperature at resolutions adequate for district-level aggregation over the same period.

This paper uses those developments to ask a narrow, testable question: does the joint occurrence of moisture deficit and heat during the growing season predict lean-season food insecurity in Zimbabwe better than moisture deficit alone?

This manuscript is a preprint and has not been peer reviewed. The copyright holder has made the manuscript available under a Creative Commons Attribution 4.0 International (CC BY) license and consented to have it forwarded to EarthArXiv for public posting.

We make four contributions. We provide, to our knowledge, the first panel test of compound drought-heat effects on food security outcomes in southern Africa. We evaluate the models on out-of-sample predictive error rather than in-sample fit alone, which is the standard an early warning application would have to meet. We show that a weak national pooled estimate conceals a strong compound effect in the driest third of districts, one that survives spatially robust inference and differs from the wettest third in a formal test, and we translate the fitted relationships into indicative CMIP6 scenario projections for the 2050s. Finally, we released the full country-parameterized pipeline. Administrative boundaries are fetched automatically, and the map projection is refitted, so replication across any of the 20 countries covered by HFID requires only setting the country code and, for countries with bimodal rainfall, redefining the seasonal windows.

2. Data

2.1 Study area

Zimbabwe is situated in southern Africa, bordered by Zambia, Mozambique, South Africa and Botswana (Figure 1). Zimbabwe covers approximately 390,000 km² between latitudes 15.6°S and 22.4°S, divided administratively into 10 provinces and 60 rural districts, and agro-ecologically into five Natural Regions defined principally by rainfall reliability. The outcome geometry used in this study (Section 2.2) comprises 84 FEWS NET units: the rural districts plus the cities and urban councils that FEWS NET reports separately (for example Harare, Bulawayo, Chitungwiza, Epworth and Beitbridge Urban). This is why the panel contains more units than there are rural districts. Natural Region I, confined to the Eastern Highlands, receives over

This manuscript is a preprint and has not been peer reviewed. The copyright holder has made the manuscript available under a Creative Commons Attribution 4.0 International (CC BY) license and consented to have it forwarded to EarthArXiv for public posting.

1,000 mm annually and supports specialized and diversified farming. Natural Regions IV and V, covering the southern lowveld and the Zambezi valley, receive under 650 mm with high inter-annual variability and are classified as suitable primarily for extensive livestock production, yet they carry substantial communal-area populations who cultivate maize regardless. This mismatch between agro-ecological suitability and actual land use is the central structural vulnerability in Zimbabwean rural food security and motivates the heterogeneity analysis in Section 3.5. District rainfall and temperature gradients provide the climatic context for the analysis (Figure 2). Administrative boundaries for display are taken from geoBoundaries (gbOpen, CC BY 4.0), which publishes openly licensed admin layers; the analysis itself remains keyed to the geometry on which the outcome is measured.

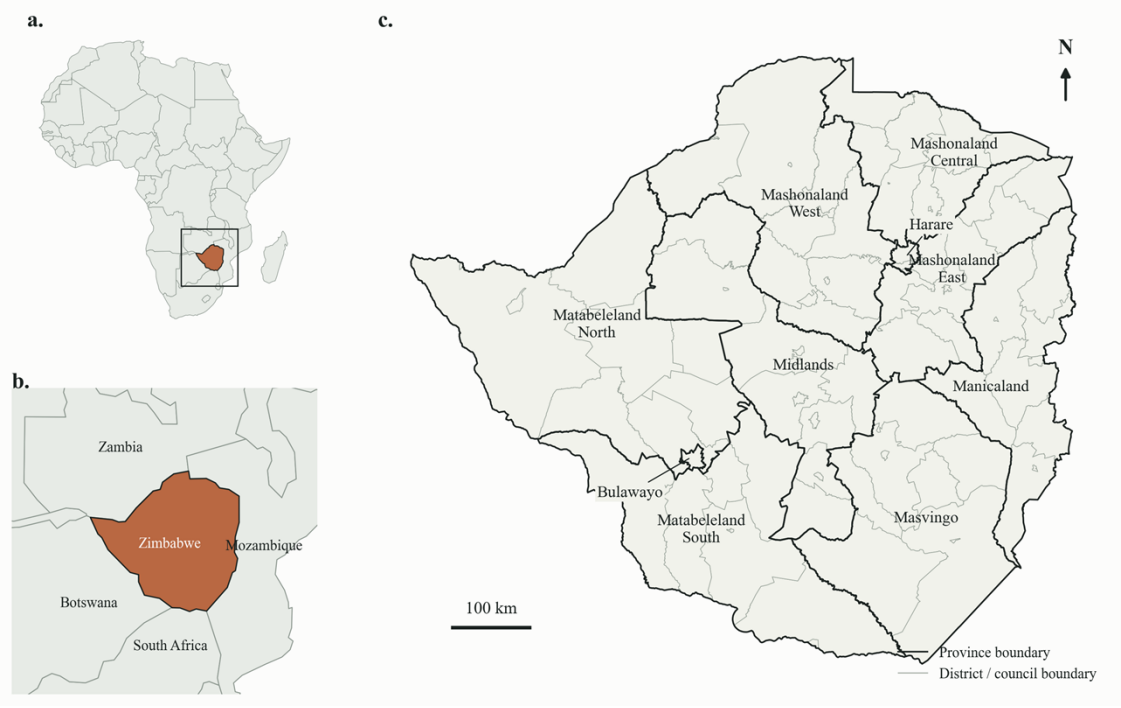


Figure 1. Location of the study area. (a) Zimbabwe within Africa. (b) Regional context. (c) Provinces and district/council boundaries, shown in an Albers equal-area projection. Administrative boundaries: geoBoundaries gbOpen (CC BY 4.0); continental and regional context: Natural Earth 1:110 million, public domain.

This manuscript is a preprint and has not been peer reviewed. The copyright holder has made the manuscript available under a Creative Commons Attribution 4.0 International (CC BY) license and consented to have it forwarded to EarthArXiv for public posting.

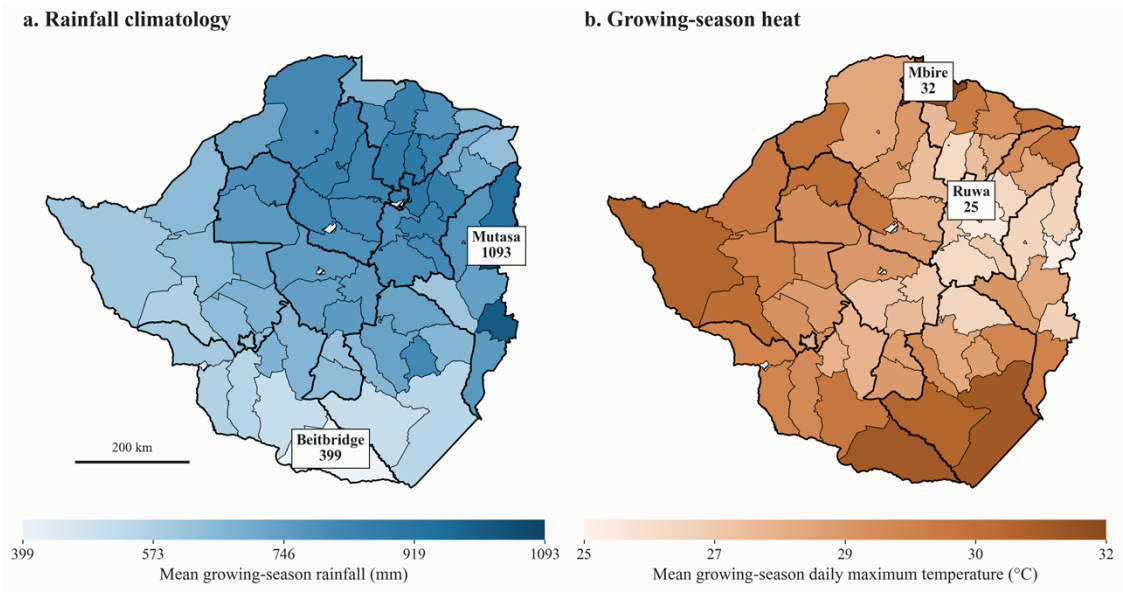


Figure 2. Zimbabwe climate gradients. (a) Mean growing-season rainfall by district. (b) Mean growing-season daily maximum temperature. Province boundaries in grey. Albers equal-area projection. Boundaries: geoBoundaries gbOpen (CC BY 4.0).

2.2 Food insecurity outcome

The outcome is the IPC-compatible area phase classification from HFID, which harmonizes IPC, Cadre Harmonisé and FEWS NET outputs onto consistent sub-national units and a monthly time step from 2009. We retain only current-situation classifications and discard the ML1 and ML2 forward projections. This is a substantive choice, not housekeeping: projections embed the analyst's own expectation of the coming rainfall season, so using them as an outcome would make the dependent variable partly a function of the independent variable.

We aggregate to a district by season-year outcome by taking the mean phase across the January to March lean season. A secondary binary outcome, whether the district reached Phase 3 or above at any point in that window, is used for robustness. Figure

This manuscript is a preprint and has not been peer reviewed. The copyright holder has made the manuscript available under a Creative Commons Attribution 4.0 International (CC BY) license and consented to have it forwarded to EarthArXiv for public posting.

3 shows how the national population-weighted mean phase and the share of districts classified as compound drought-heat have moved across the full record.

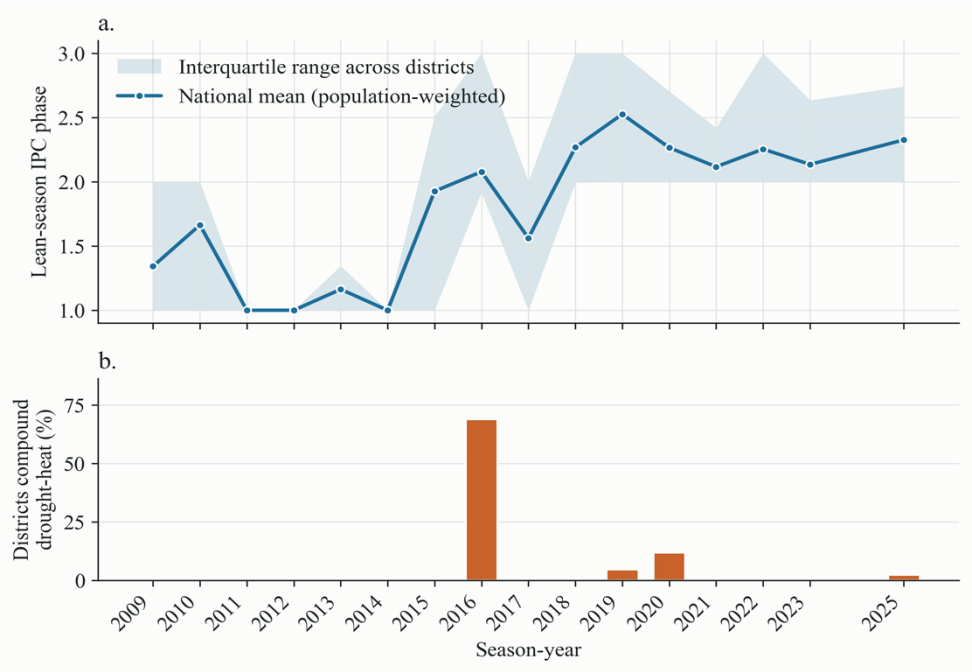


Figure 3. National record, 2009-2025. (a) Mean lean-season IPC phase, population-weighted, with the interquartile range across districts shaded. (b) Share of districts classified as compound drought-heat each season.

2.3 Exposure

i. **Rainfall.** CHIRPS version 3 daily reanalysis (dataset *UCSB-CHC/CHIRPS/V3/DAILY_RNL*), 0.05° resolution, 1981 to present. Version 3 supplies two streams, an ERA5-based reanalysis and an IMERG-based near-real-time product; we use the reanalysis stream throughout because mixing them would introduce a discontinuity in the middle of the series.

ii. **Temperature.** ERA5-Land daily aggregates (dataset *ECMWF/ERA5_LAND/DAILY_AGGR*), 0.1° resolution, providing daily maximum and minimum 2 m air temperature.

This manuscript is a preprint and has not been peer reviewed. The copyright holder has made the manuscript available under a Creative Commons Attribution 4.0 International (CC BY) license and consented to have it forwarded to EarthArXiv for public posting.

Both are reduced to district means in Google Earth Engine against the FEWS NET boundary geometry, so exposure and outcome are defined on identical units. This avoids the areal interpolation error that would arise from extracting against GADM or GAUL units and then cross-walking by name. Figure S1 shows the descriptive growing-season rainfall and temperature trend over the record; because the two-way fixed effects model absorbs any trend common across districts, this is context rather than the paper's estimates. Figure 4 and Figure 5 show the underlying continuous rainfall and temperature surfaces by period, as native-resolution gridded fields rather than a district choropleth, and before either is standardized or classified.

This manuscript is a preprint and has not been peer reviewed. The copyright holder has made the manuscript available under a Creative Commons Attribution 4.0 International (CC BY) license and consented to have it forwarded to EarthArXiv for public posting.

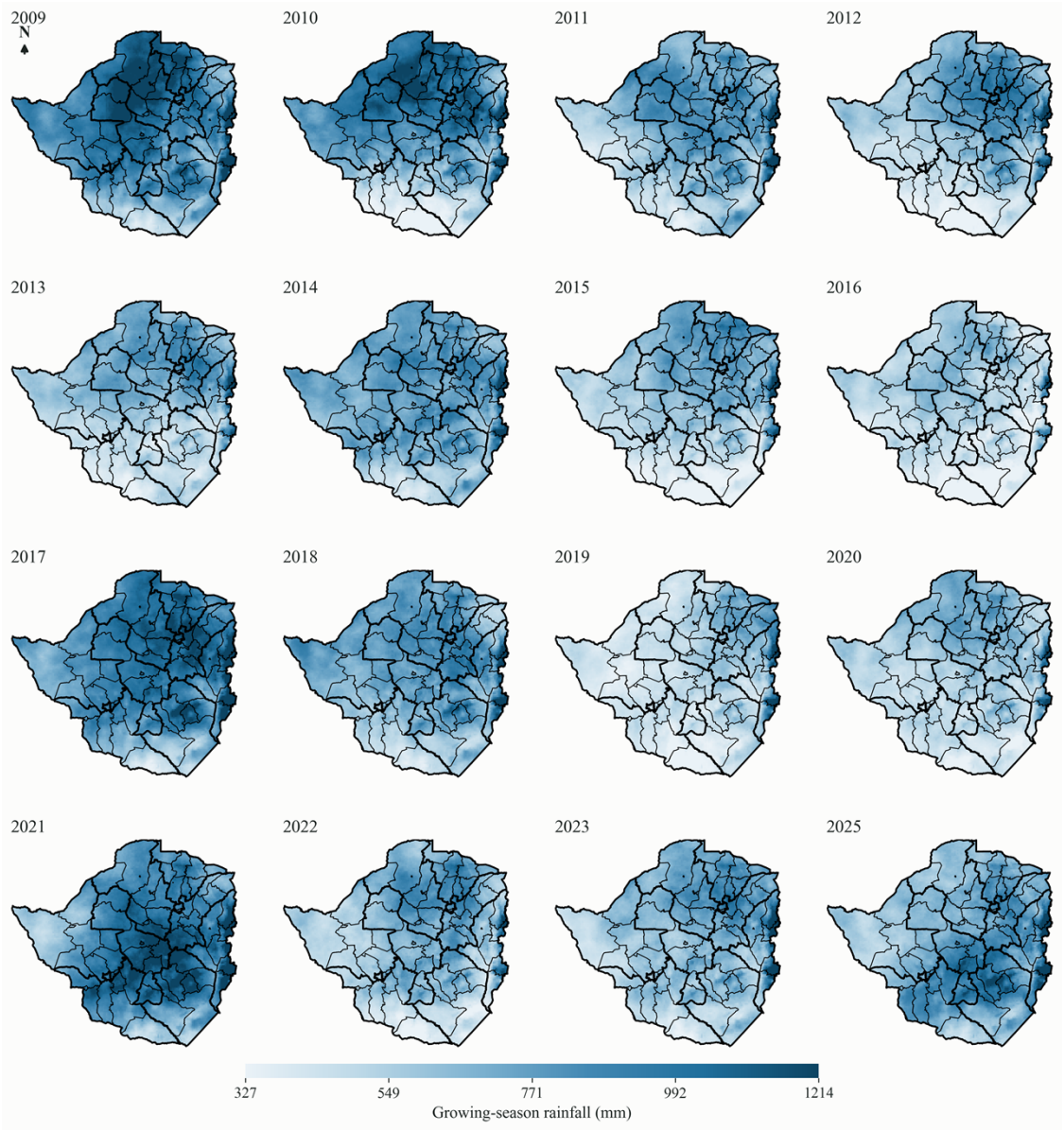


Figure 4. Growing-season rainfall by period, the raw continuous exposure variable, prior to any standardization or drought classification. Native 5.6 km CHIRPS v3 grid, not a district choropleth; boundaries shown for reference only. Small multiples on one shared color scale.

This manuscript is a preprint and has not been peer reviewed. The copyright holder has made the manuscript available under a Creative Commons Attribution 4.0 International (CC BY) license and consented to have it forwarded to EarthArXiv for public posting.

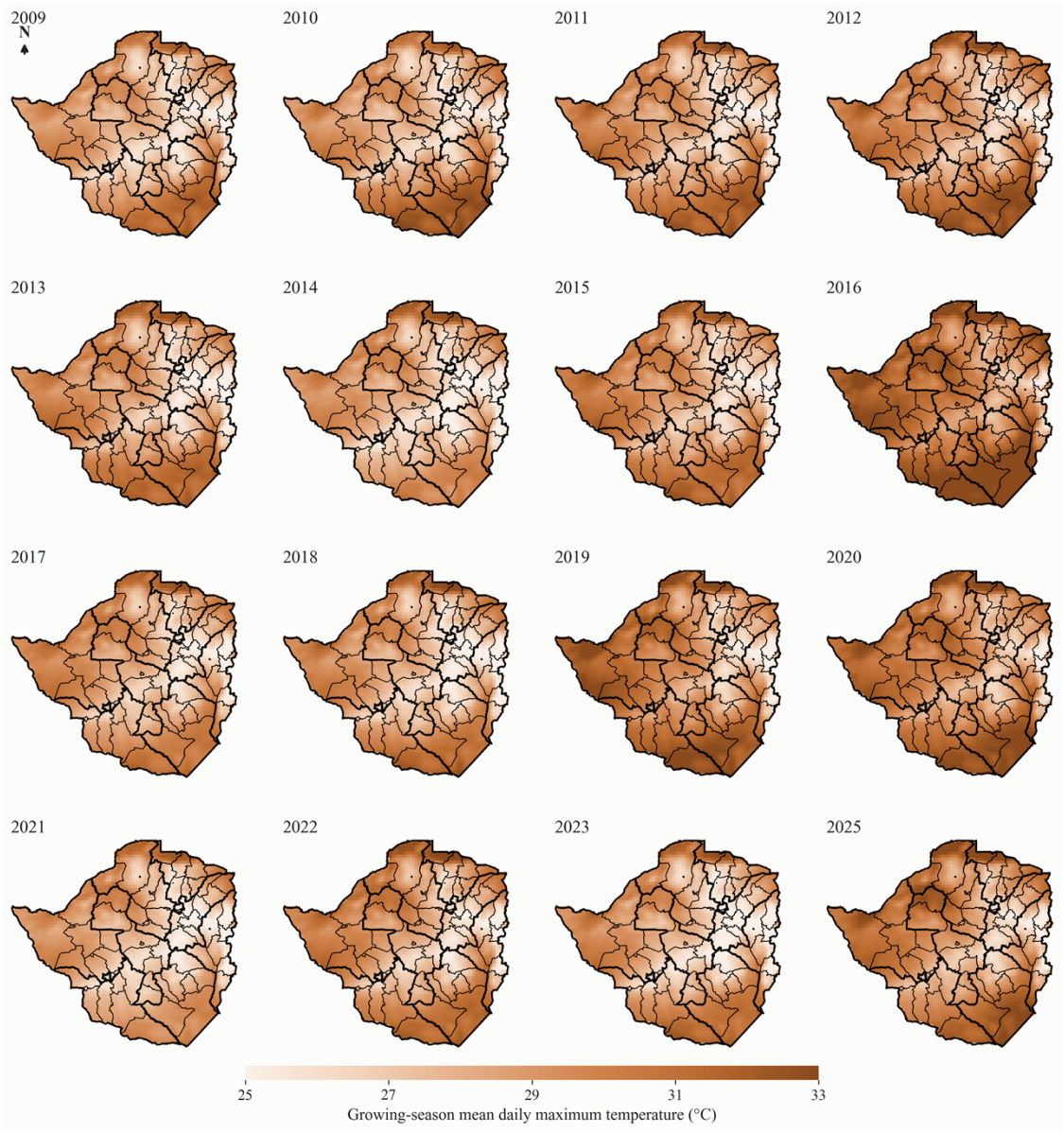


Figure 5. Growing-season means daily maximum temperature by period, the raw continuous exposure variable, prior to any hot-day thresholding. Native 11.1 km ERA5-Land grid, not a district choropleth; boundaries shown for reference only. Same period bins and color-scale convention as the rainfall-by-period figure.

2.4 Temporal alignment

Season-year *Y* spans October of *Y-1* through March of *Y*, with harvest in April and May of *Y*. The outcome for season-year *Y* is measured in the lean season of *Y+1*, which is the period the harvest of year *Y* must carry households through. Exposure

This manuscript is a preprint and has not been peer reviewed. The copyright holder has made the manuscript available under a Creative Commons Attribution 4.0 International (CC BY) license and consented to have it forwarded to EarthArXiv for public posting.

therefore precedes outcome by nine to fourteen months, and the ordering is fixed by the agricultural calendar rather than chosen to fit (Figure S2).

3. Methods

3.1 Moisture deficit

We compute monthly potential evapotranspiration by the Hargreaves-Samani method from district daily temperature extremes and latitude-derived extraterrestrial radiation. Hargreaves is chosen over Penman-Monteith deliberately: it requires only temperature, so it draws on the same extraction as the heat variables and does not import wind and radiation products with different and uncharacterized error structures over Zimbabwe.

The monthly climatic water balance is $D = P - PET$. We accumulate D over six months ending in March, capturing the full growing season, and standardise within each district and calendar month using the Gringorten plotting position. We use the nonparametric standardization rather than fitting a three-parameter log-logistic distribution because the 45-year record makes parametric fits unstable in the driest districts; the parametric alternative is implemented and reported as a robustness check. The result is SPEI-6 at season end. A rainfall-only comparator, SPI-6, is constructed identically on precipitation alone

.

SPEI's value over SPI specifically in this region is not only theoretical. Manatsa, Mushore and Lenouo (2017) validate SPEI directly against southern African drought outcomes and tie it to ENSO forcing, the same mechanism behind the 2015/16 season this paper discusses in Section 5; a rainfall-only index misses that link, which

This manuscript is a preprint and has not been peer reviewed. The copyright holder has made the manuscript available under a Creative Commons Attribution 4.0 International (CC BY) license and consented to have it forwarded to EarthArXiv for public posting.

is part of the physical case in Section 1 for why the moisture term used here already carries information a precipitation anomaly alone would not.

3.2 Heat

A hot day is a growing-season day on which district mean daily maximum temperature exceeds that district's own 90th percentile of growing-season daily maxima over the 1991 to 2020 WMO normal period. The threshold is district-specific because an absolute cut would simply re-encode the latitudinal temperature gradient, which the district fixed effect already absorbs. The heat exposure variable is the count of such days per growing season. Figure S3 and Figure S4 show these two standardized indices, moisture deficit and heat exposure, as continuous district-level quantities by period, before either is reduced to the binary threshold below.

3.3 Compound specification

We report two operationalization's side by side, because the compound event literature has not converged on a single operationalization and a referee will ask about whichever is omitted.

i. **Continuous.** Both exposures are standardized within district, so coefficients are interpreted relative to that district's own normal conditions. The compound term is their product, the standardized moisture deficit multiplied by the standardized hot-day count.

ii. **Binary.** A drought season is SPEI-6 below -0.8, the McKee moderate-drought threshold. A hot season is a hot-day count above the district's own 80th

This manuscript is a preprint and has not been peer reviewed. The copyright holder has made the manuscript available under a Creative Commons Attribution 4.0 International (CC BY) license and consented to have it forwarded to EarthArXiv for public posting.

267 percentile. The compound indicator is their intersection, estimated alongside
268 drought-only and heat-only indicators against a neither-hazard reference.

269 **3.4 Estimation**
270 The primary specification is two-way fixed effects:

271 $$y_{dt} = \beta_1 \cdot dry_{dt} + \beta_2 \cdot heat_{dt} + \beta_3 \cdot (dry \times heat)_{dt} + \alpha_d + \delta_t + \varepsilon_{dt}$$

272 where y is mean lean-season IPC phase, α_d is a district fixed effect and δ_t a season-
273 year fixed effect. Standard errors are clustered at district. The design follows
274 Schlenker and Lobell's (2010) panel treatment of nonlinear heat exposure in African
275 agriculture, extended here with an explicit interaction term rather than an additive
276 one.

277

278 The district fixed effect absorbs all time-invariant district characteristics, which is why
279 time-invariant vulnerability covariates such as market access, soil quality and Natural
280 Region do not appear as controls: they are differenced out. The year fixed effect
281 absorbs national shocks common to all districts, including macroeconomic
282 conditions, currency changes, national policy and the pandemic. Identification
283 therefore comes from within-district deviations from a district's own seasonal norms,
284 relative to the national average deviation that year.

285

286 Models are estimated as a nested ladder: rainfall only (M1), SPEI only (M2), SPEI
287 plus heat additively (M3), the full compound interaction (M4), and the binary
288 categorical version (M5).

This manuscript is a preprint and has not been peer reviewed. The copyright holder has made the manuscript available under a Creative Commons Attribution 4.0 International (CC BY) license and consented to have it forwarded to EarthArXiv for public posting.

3.5 Model comparison and heterogeneity

In-sample comparison uses within-R^2, computed on the two-way demeaned data so that it is the share of within-district, within-season variation explained, together with the log-likelihood. The more demanding test is leave-one-season-out cross-validation: each season-year is held out in turn, the model refitted, and the held-out season predicted using district intercepts and slopes only. The year effect is unavailable out of sample, which is the honest forecasting position, since an operational system predicting the coming lean season does not know that season's national shock. We report RMSE, MAE and skill relative to a training-mean baseline. Random k-fold cross-validation is deliberately avoided: it would leak same-year information across districts through the year effect and flatter every specification equally.

Heterogeneity is tested two ways. The compound specification is estimated separately within each agro-ecological stratum, which keeps each estimate an internally valid within estimator but does not license formal comparison between strata. A pooled model interacting the compound term with stratum indicators is therefore reported alongside, and it is that model, not the split samples, that tests whether the effect differs.

Where the authoritative Natural Region boundary file is available, strata are Natural Regions I to V, with districts spanning more than one region assigned their modal region by cropped area. Where it is not, the pipeline substitutes terciles of each district's own growing-season rainfall climatology and says so explicitly. The tercile

This manuscript is a preprint and has not been peer reviewed. The copyright holder has made the manuscript available under a Creative Commons Attribution 4.0 International (CC BY) license and consented to have it forwarded to EarthArXiv for public posting.

version is a defensible aridity stratified, but it is not the Natural Region classification and is not described as one.

3.6 Inference

Clustering at district permits arbitrary serial correlation within a district but imposes independence across districts. That assumption is untenable for weather-driven exposures, which are correlated at scales far larger than a Zimbabwean district. Year fixed effects absorb the national component of that correlation but not the regional one. We therefore report Conley (1999) spatial HAC standard errors alongside the clustered ones, using a Bartlett kernel in space with a 200 km cutoff and in time with a three-year lag. Because the cutoff is a researcher choice with no data-driven answer, we report inference across cutoffs from 100 to 500 km.

As a check with no distributional assumption at all, we also report randomization inference on the compound interaction: within each district independently, the season-year assignment of the three exposure terms is permuted while the outcome is held fixed, so each district's own marginal distribution of moisture deficit, heat and their product is preserved exactly and only the true season-to-season pairing with that district's own outcome is broken. The model is re-estimated on each of 500 such permutations, giving an empirical null distribution for the compound coefficient against which the observed estimate is compared directly, with no reliance on asymptotic normality. Because permuting each district independently also breaks the cross-district dependence of weather shocks, we add a season-block permutation that reassigns whole season-years jointly across all districts (1,000 permutations).

This manuscript is a preprint and has not been peer reviewed. The copyright holder has made the manuscript available under a Creative Commons Attribution 4.0 International (CC BY) license and consented to have it forwarded to EarthArXiv for public posting.

This keeps each season's spatial pattern of exposure intact, so it tests a null comparable to the one behind the Conley errors.

3.7 Rainfall product sensitivity

Zimbabwe's rain gauge network has thinned since 2000, so satellite rainfall skill is not constant across the study period, and no product can be treated as ground truth. We re-estimate the full model ladder on an independent rainfall product and compare. The available alternative in the same extraction is ERA5-Land precipitation, which is model reanalysis: independent of CHIRPS in lineage but known to be wet-biased over southern Africa. It therefore tests robustness to product choice rather than establishing accuracy. A stronger check, using the gauge-calibrated TAMSAT product, requires a separate download and is noted as such.

3.8 Climate-change scenario projection

The fitted model describes an association recovered from 2009-2025. Extending it forward requires future climate data, which this pipeline does not otherwise use, and a decision about how to combine a climate model's own biases with an already-fitted statistical relationship. We use a delta method, standard in agricultural climate-impact assessment for exactly this situation: only the *change* a climate model projects are trusted, not its absolute level, and that change is applied on top of our own observed CHIRPS/ERA5-Land climatology rather than replacing it.

Growing-season total rainfall and mean daily maximum temperature, from the NASA NEX-GDDP-CMIP6 ensemble (30 of its 33 models; three do not report daily

This manuscript is a preprint and has not been peer reviewed. The copyright holder has made the manuscript available under a Creative Commons Attribution 4.0 International (CC BY) license and consented to have it forwarded to EarthArXiv for public posting.

maximum temperature and are excluded from both variables' ensembles for consistency), under two Shared Socioeconomic Pathways, SSP2-4.5 (moderate mitigation) and SSP5-8.5 (high emissions), for 2046-2065 ("the 2050s"), against the ensemble's own 1995-2014 historical reference period. One horizon rather than a full multi-horizon sweep is a deliberate scope choice.

Rather than assume a parametric response, the projected rainfall and temperature change is mapped through each district's own *historical, empirical* relationship between its climate and its standardized exposure variables, so the projection uses exactly the standardization the model was fitted on (Section 3.1-3.2), not a new assumption layered on top. For moisture: the projected water-balance shift is interpolated against each district's own historical (water balance, dry_z) pairs. For heat: each district's hot-day count under the shifted climate is recomputed empirically from its own real historical daily temperature record, by re-applying the district's fixed hot-day threshold shifted by the projected temperature change: exactly equivalent to shifting the future daily distribution and recounting against the original threshold, with no assumption about the distribution's shape. The resulting exposure shift is then evaluated through the same fitted coefficients as the rest of the paper (the stratum-specific coefficients of Section 3.5 where a district's stratum has one, the pooled coefficients otherwise), giving a projected change in mean lean-season phase per district per scenario.

Two simplifying assumptions are made explicitly, not left implicit. First, the daily minimum temperature is assumed to shift by the same amount as the maximum (the

This manuscript is a preprint and has not been peer reviewed. The copyright holder has made the manuscript available under a Creative Commons Attribution 4.0 International (CC BY) license and consented to have it forwarded to EarthArXiv for public posting.

diurnal range is unchanged), which gives the potential evapotranspiration response to warming in closed form from the Hargreaves formula itself (Section 3.1) rather than requiring a second, independently projected variable. Second, population is held at its currently reported level in every scenario: this is a climate-only projection, not a combined climate and demographic projection, and is reported as such wherever a population appears.

4. Results

4.1 Panel description

The analysis panel comprises 1,342 district-seasons across 84 district and urban-council units and 16 seasons (2009 to 2025). Mean lean-season phase is 1.82. Compound drought-heat seasons under the binary definition account for 5.5% of district-seasons.

4.2 Nested model ladder

All five specifications are estimated on the same 1,342 district-seasons. Within-R^2 rises from 0.0015 in the SPEI-only model to 0.0022 with an additive heat term and 0.0045 with the compound interaction, and the log-likelihood rises in the same order (-760.6, -760.2, -758.6); the rainfall-only model gives 0.0023 (Table 1, Figure 6). The explained shares are small because the season-year fixed effect absorbs the national component of climate variation.

The interaction coefficient is +0.030 (SE 0.017, p = 0.083).

This manuscript is a preprint and has not been peer reviewed. The copyright holder has made the manuscript available under a Creative Commons Attribution 4.0 International (CC BY) license and consented to have it forwarded to EarthArXiv for public posting.

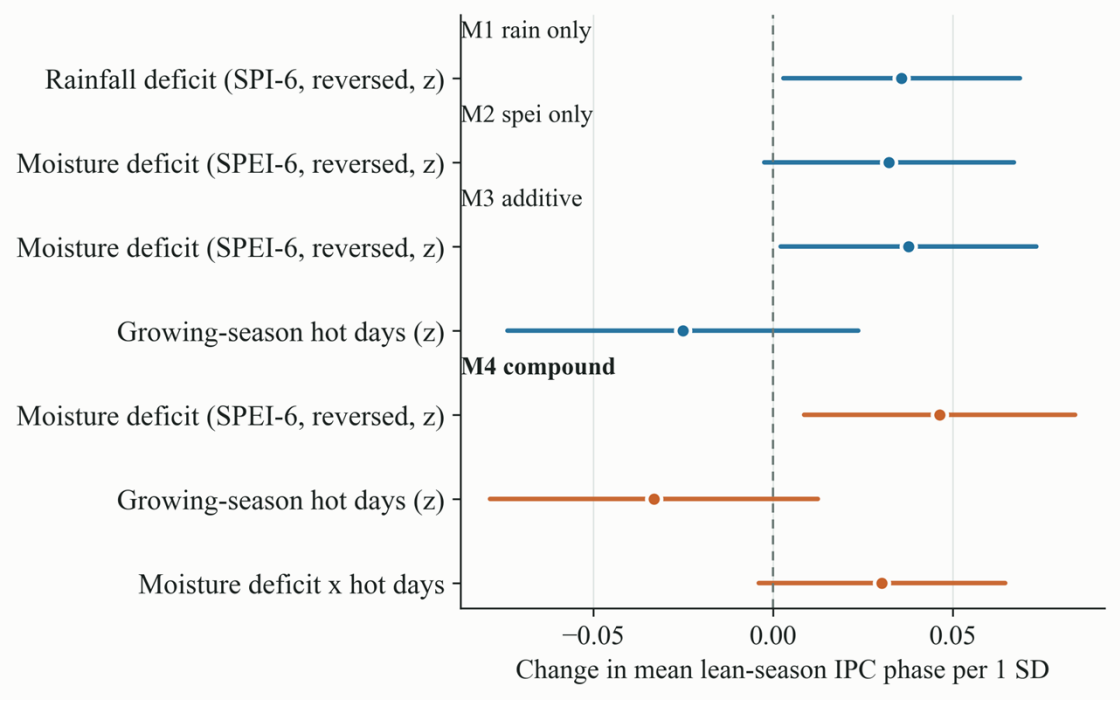


Figure 6. Nested model ladder. Point estimates with 95 per cent confidence intervals, clustered at district. The compound specification is highlighted.

Table 1. Nested model ladder: coefficients, standard errors clustered at district. All models: N = 1,342 district-seasons, 84 units, 16 seasons.

model	term	coef	se	p
M1_rain_only	Rainfall deficit (SPI-6, reversed, z)	0.0358	0.0168	0.033
M2_spei_only	Moisture deficit (SPEI-6, reversed, z)	0.0322	0.0177	0.069
M3_additive	Moisture deficit (SPEI-6, reversed, z)	0.0377	0.0181	0.037
M3_additive	Growing-season hot days (z)	-0.0250	0.0248	0.314
M4_compound	Moisture deficit (SPEI-6, reversed, z)	0.0463	0.0192	0.016
M4_compound	Growing-season hot days (z)	-0.0331	0.0232	0.154

This manuscript is a preprint and has not been peer reviewed. The copyright holder has made the manuscript available under a Creative Commons Attribution 4.0 International (CC BY) license and consented to have it forwarded to EarthArXiv for public posting.

model	term	coef	se	p
M4_compound	Moisture deficit x hot days	0.0303	0.0175	0.083
M5_binary	Drought, not hot	0.1165	0.0902	0.197
M5_binary	Hot, not drought	-0.0424	0.0412	0.304
M5_binary	Compound drought-heat	-0.0635	0.1055	0.547

4.3 Marginal effect of moisture deficit across heat conditions

The model-based marginal effect is shown first (Figure 7); the binned figure that follows it (Figure S5) gives the same result without imposing a functional form, by splitting the sample into heat terciles and plotting two-way demeaned outcomes against two-way demeaned moisture deficit. If the interaction is an artefact of the linear specification, the binned slopes will not steepen.

The effect of a one standard deviation moisture deficit on mean lean-season phase is -0.014 phase points in a season two standard deviations cooler than the district norm and +0.107 phase points in a season two standard deviations hotter, so the effect is indistinguishable from zero, or reversed, in cool seasons and appears only as the season warms.

This manuscript is a preprint and has not been peer reviewed. The copyright holder has made the manuscript available under a Creative Commons Attribution 4.0 International (CC BY) license and consented to have it forwarded to EarthArXiv for public posting.

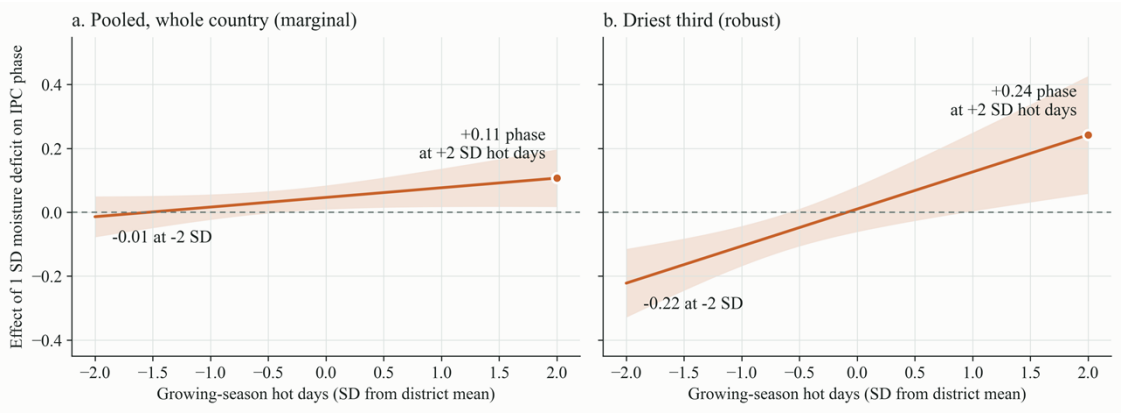


Figure 7. Marginal effect of a one standard deviation moisture deficit on mean lean-season IPC phase, across growing-season heat conditions, 95 per cent confidence band. Where the pooled, whole-country estimate is not itself the strongest available (Section 4.7), shown alongside the same estimate within the stratum where the compound interaction is largest and individually significant, on a shared axis.

4.4 Categorical decomposition

Relative to seasons with neither hazard, drought-only seasons show +0.116 phase points, heat-only seasons -0.042 phase points, and compound seasons -0.064 phase points (Figure 8). The compound coefficient does not exceed the sum of the single-hazard coefficients (-0.064 against +0.074), so the effect is additive rather than super-additive on this definition. With compound seasons making up only 5.5 per cent of district-seasons (about 74 observations), however, the binary contrast is imprecise (95 per cent CI approximately −0.27 to +0.14) and cannot discriminate between additive and interactive effects; the continuous specification is the more informative test.

The geographic pattern is mapped alongside (Figure 9), so the reader can see whether compound exposure and poor outcomes coincide in space rather than only in the regression; Figure S6 separates the two component hazards, Figure S7 and

This manuscript is a preprint and has not been peer reviewed. The copyright holder has made the manuscript available under a Creative Commons Attribution 4.0 International (CC BY) license and consented to have it forwarded to EarthArXiv for public posting.

Figure S8 give the same two variables by period, and Figure S9 shows the full district-by-season record at once.

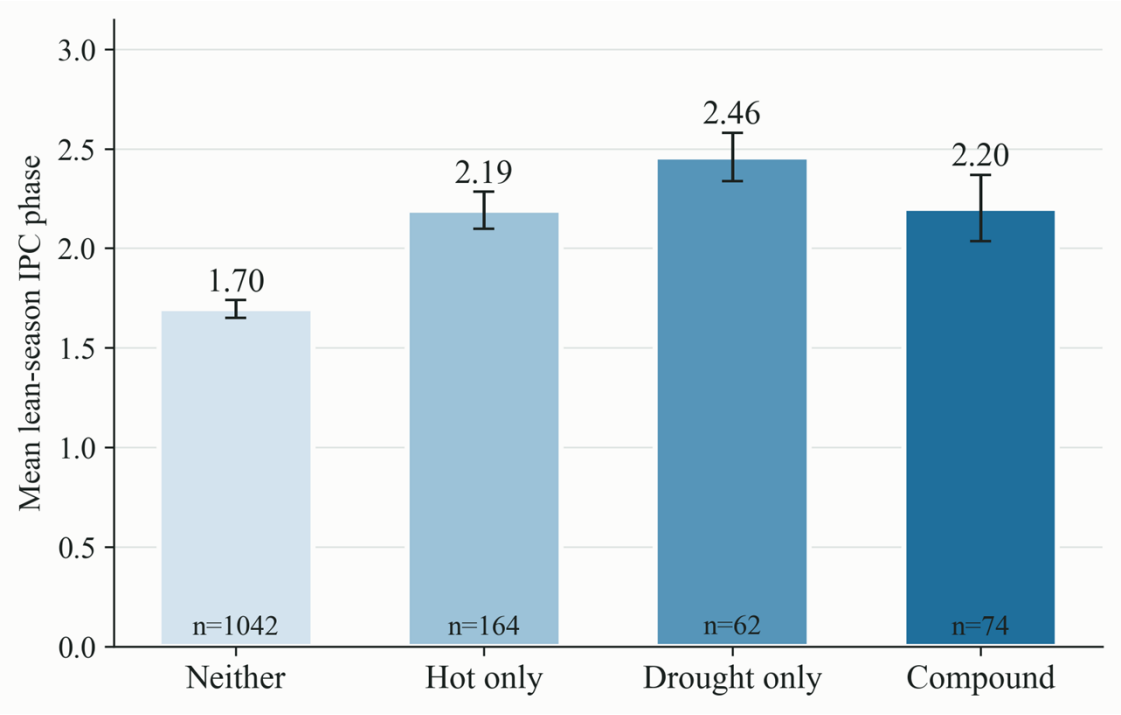


Figure 8. Mean lean-season IPC phase by drought and heat co-occurrence, with 95 per cent confidence intervals. Categories are ordered by expected severity.

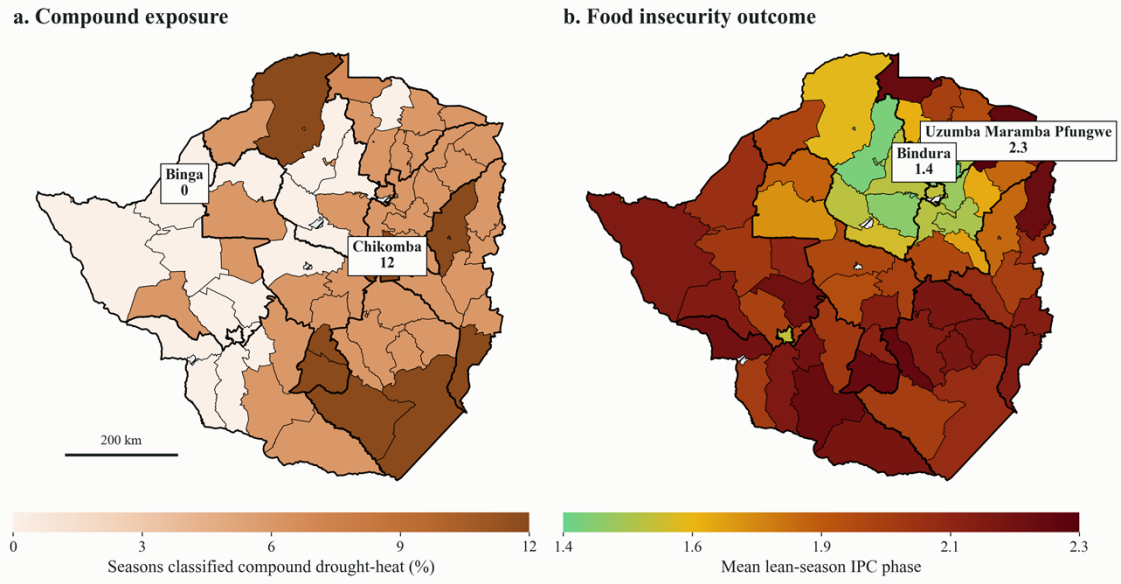


Figure 9. Geographic pattern. (a) Share of seasons classified as compound drought-heat. (b) Mean lean-season IPC phase. Hatched units carry no outcome data.

This manuscript is a preprint and has not been peer reviewed. The copyright holder has made the manuscript available under a Creative Commons Attribution 4.0 International (CC BY) license and consented to have it forwarded to EarthArXiv for public posting.

4.5 Out-of-sample prediction

Leave-one-season-out RMSE is 0.732 for the rainfall-only model and 0.748 for the compound model, so the compound model is 2.2 per cent worse out of sample (Figure 10, Table 2). The binary specification (M5) has the lowest out-of-sample error (RMSE 0.695; 9.4 per cent skill relative to the training mean), but all specifications explain only a small share of lean-season variation once the national year effect is unavailable, underlining that climate exposure alone is an incomplete basis for forecasting food-security outcomes.

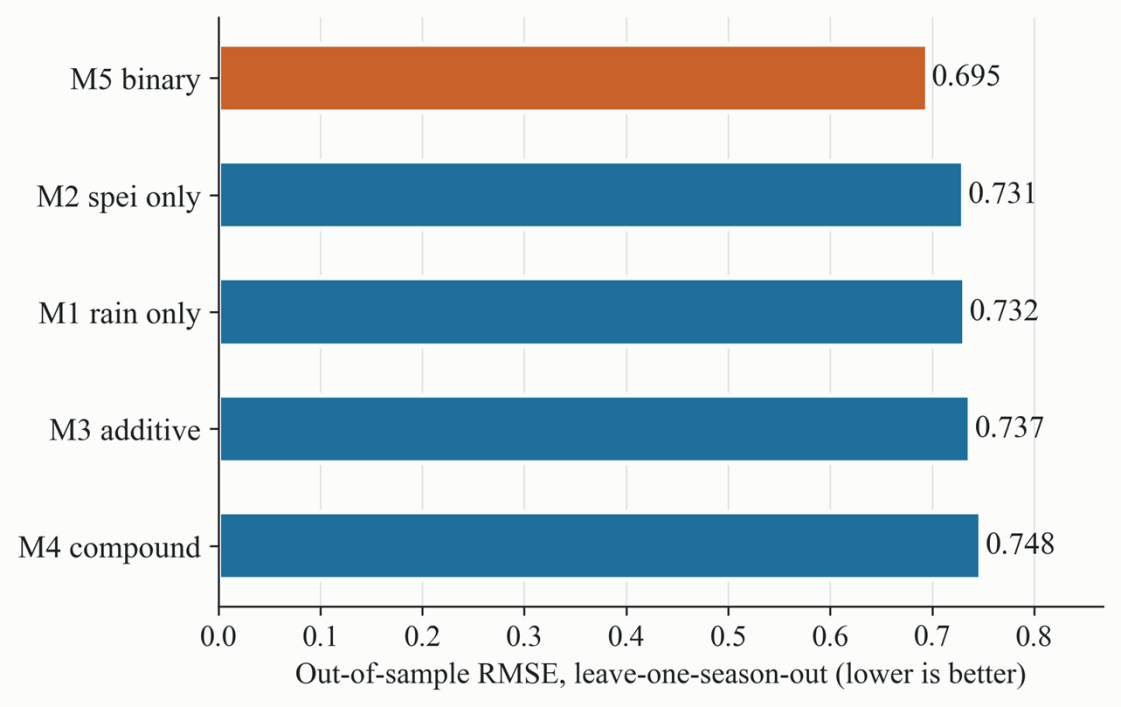


Figure 10. Leave-one-season-out root mean squared error by specification. Lower is better. The held-out season is predicted from district intercepts and slopes only.

This manuscript is a preprint and has not been peer reviewed. The copyright holder has made the manuscript available under a Creative Commons Attribution 4.0 International (CC BY) license and consented to have it forwarded to EarthArXiv for public posting.

Table 2. Leave-one-season-out predictive performance.

model	n pred	rmse	mae	rmse skill vs means
M5_binary	1342	0.6953	0.5907	0.0937
M2_spei_only	1342	0.7307	0.6277	0.0476
M1_rain_only	1342	0.7320	0.6287	0.0459
M3_additive	1342	0.7374	0.6287	0.0388
M4_compound	1342	0.7479	0.6343	0.0251

4.6 Robustness

Across the three alternative specifications (district-only fixed effects, exclusion of the pandemic years, and a linear probability model on the crisis indicator), the interaction keeps its positive sign in every case but is statistically significant only with district-only fixed effects ($p = 0.003$), the least credible specification of the set because it does not absorb common national shocks (Table 3).

Table 3. Robustness of the compound interaction across specifications.

variant	n	dry z	heat z	interaction	p interaction
Main (district + year FE)	1342	0.0463	-0.0331	0.0303	0.083
District FE only	1342	0.1004	0.0881	0.0311	0.003
Excluding COVID years	1174	0.0571	-0.0304	0.0165	0.386
Outcome = crisis indicator (LPM)	1342	-0.0259	-0.0064	0.0195	0.154

4.7 Heterogeneity across agro-ecological strata

Strata are defined by terciles of district growing-season rainfall climatology (the Natural Region boundary file was not available, so these are an aridity proxy, not

This manuscript is a preprint and has not been peer reviewed. The copyright holder has made the manuscript available under a Creative Commons Attribution 4.0 International (CC BY) license and consented to have it forwarded to EarthArXiv for public posting.

Natural Regions) (Figure 11). The compound interaction ranges from +0.013 to +0.116 across the 3 strata and is individually significant in 1 of them. The pooled three-way model, which is what formally tests difference, shows that the compound interaction in the driest third exceeds that in the wettest third by +0.051 (SE 0.024, p = 0.029); the middle third does not differ from the wettest (+0.036, SE 0.029, p = 0.219), and the joint Wald test that neither differs gives $\chi^2(2) = 4.87$, p = 0.087 (Table 4 note). The driest-third estimate also survives the two checks that remove the pooled result: its Conley p is below 0.001 at every cutoff from 100 to 500 km, and the season-block permutation gives p = 0.004 (1,000 permutations). The effect is concentrated rather than uniform, and pooling the whole country understates it where it operates. (Figure 12, Table 4)

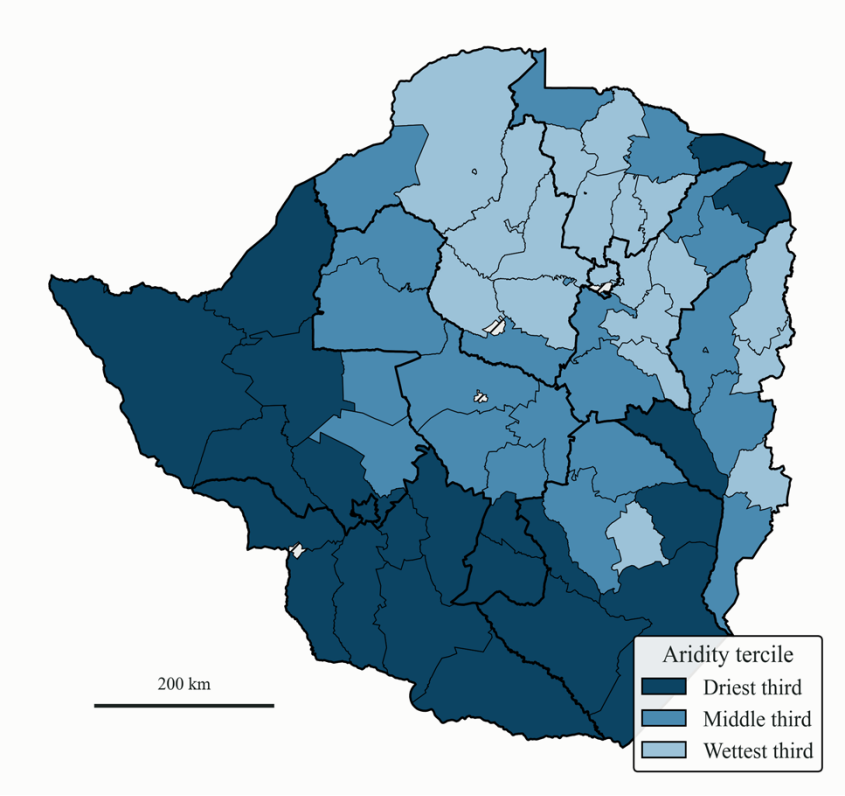


Figure 11. Agro-ecological stratification is used in the heterogeneity analysis above.

This manuscript is a preprint and has not been peer reviewed. The copyright holder has made the manuscript available under a Creative Commons Attribution 4.0 International (CC BY) license and consented to have it forwarded to EarthArXiv for public posting.

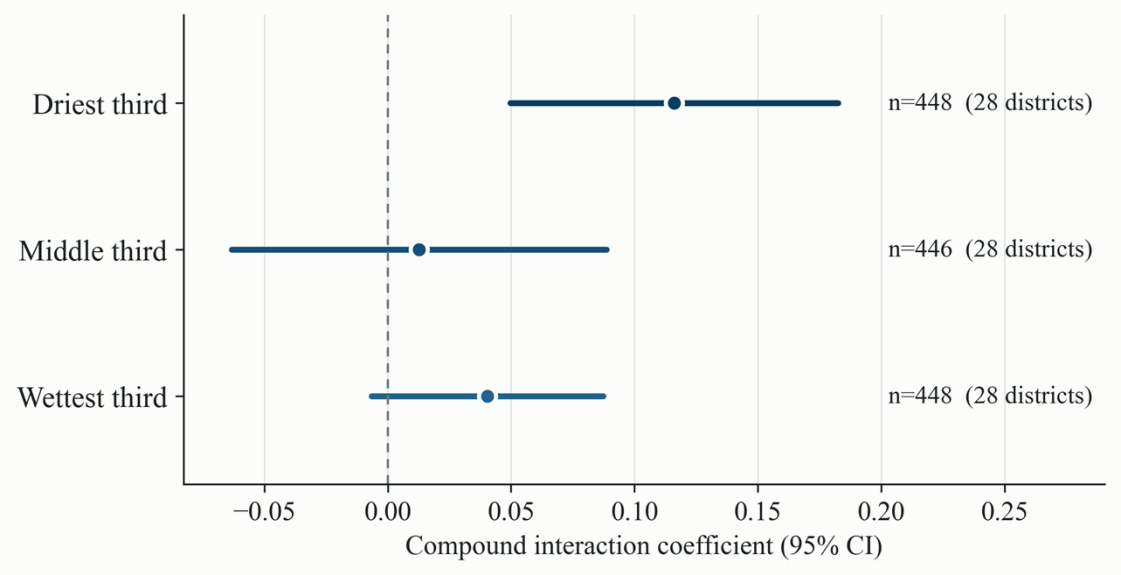


Figure 12. Compound interaction is estimated separately within each agro-ecological stratum, with 95 per cent confidence intervals and sample sizes.

Table 4. Compound specification is estimated within agro-ecological strata.

stratum	n	n districts	dry z	heat z	interaction	se interaction	p interaction	within r2
Driest third	448	28	0.0100	0.1313	0.1161	0.0339	< 0.001	0.0391
Middle third	446	28	0.0061	-0.0080	0.0128	0.0387	0.742	0.0005
Wettest third	448	28	0.0781	-0.0258	0.0403	0.0239	0.093	0.0100

Note. Within-R^2 is computed on the two-way demeaned data. Pooled three-way test (all 1,342 district-seasons, wettest third as reference): difference in the compound interaction, driest minus wettest third, +0.051 (SE 0.024, p = 0.029); middle minus wettest, +0.036 (SE 0.029, p = 0.219); joint Wald test that both differences are zero, $\chi^2(2) = 4.87$, p = 0.087. Driest third against the other two thirds combined: +0.033 (SE 0.022, p = 0.132). Driest-third interaction under Conley errors: p < 0.001 at every cutoff from 100 to 500 km; season-block permutation p = 0.004.

This manuscript is a preprint and has not been peer reviewed. The copyright holder has made the manuscript available under a Creative Commons Attribution 4.0 International (CC BY) license and consented to have it forwarded to EarthArXiv for public posting.

4.8 Spatial correlation and inference

Allowing shocks to be correlated across districts within 200 km and across three years, the Conley standard error on the compound interaction is 0.0192, against 0.0175 when clustering at district alone (Figure S10, Table 5). Allowing for spatial correlation widens the interval, as expected, and the pooled interaction is not significant at any cutoff from 100 to 500 km (p from 0.105 to 0.171).

Within-district randomization inference points the other way. Across 500 permutations, each preserving a district's own marginal exposure distribution while breaking the true season-to-season pairing with its own outcome, only 1 produced a compound coefficient as large in magnitude as the observed +0.0303 (empirical two-sided p 0.002), against a null distribution centered near zero (mean +0.0000, s.d. 0.0103) (Figure S11). The two procedures test different nulls. Because exposures are permuted independently within each district, the permutation null breaks the cross-district spatial dependence of weather shocks that the Conley estimator retains and is therefore likely to understate the sampling dispersion of the coefficient under spatially correlated exposures. The season-block permutation, which retains that dependence, confirms this: its null distribution is three times wider (s.d. 0.032) and 353 of 1,000 permutations produce a coefficient at least as large in magnitude as the observed one (empirical p = 0.353), in line with the Conley result. We accordingly treat the pooled interaction as suggestive rather than established and rest the substantive conclusion on the stratified results in Section 4.7.

This manuscript is a preprint and has not been peer reviewed. The copyright holder has made the manuscript available under a Creative Commons Attribution 4.0 International (CC BY) license and consented to have it forwarded to EarthArXiv for public posting.

Table 5. Conley spatial HAC standard errors across distance cutoffs.

dist km	term	coef	se conley	p
100	dry_z	0.0463	0.0246	0.060
100	heat_z	-0.0331	0.0296	0.264
100	compound_cont	0.0303	0.0187	0.105
150	dry_z	0.0463	0.0257	0.072
150	heat_z	-0.0331	0.0320	0.301
150	compound_cont	0.0303	0.0191	0.113
200	dry_z	0.0463	0.0264	0.079
200	heat_z	-0.0331	0.0340	0.329
200	compound_cont	0.0303	0.0192	0.115
300	dry_z	0.0463	0.0267	0.082
300	heat_z	-0.0331	0.0363	0.361
300	compound_cont	0.0303	0.0194	0.118
500	dry_z	0.0463	0.0261	0.076
500	heat_z	-0.0331	0.0422	0.433
500	compound_cont	0.0303	0.0221	0.171

4.9 Rainfall product sensitivity

Re-estimating on the independent rainfall product returns a compound interaction of +0.053, against +0.030 on CHIRPS v3 (Table 6). The estimates differ materially, so the choice of rainfall product matters and the result should be reported as conditional on it.

Table 6. Model ladder re-estimated on an independent rainfall product.

model	product	term	coef	se	p
M1_rain_only	CHIRPS v3	spi_dry_z	0.0358	0.0168	0.033

This manuscript is a preprint and has not been peer reviewed. The copyright holder has made the manuscript available under a Creative Commons Attribution 4.0 International (CC BY) license and consented to have it forwarded to EarthArXiv for public posting.

model	product	term	coef	se	p
M1_rain_only	alternate	spi_dry_z	0.0072	0.0208	0.731
M4_compound	CHIRPS v3	dry_z	0.0463	0.0192	0.016
M4_compound	CHIRPS v3	heat_z	-0.0331	0.0232	0.154
M4_compound	CHIRPS v3	compound_cont	0.0303	0.0175	0.083
M4_compound	alternate	dry_z	0.0194	0.0217	0.370
M4_compound	alternate	heat_z	-0.0440	0.0241	0.068
M4_compound	alternate	compound_cont	0.0526	0.0214	0.014

4.10 Climate-change scenario projection

Under SSP245 by the 2050s, the population-weighted mean change in lean-season IPC phase is a rise of 0.091, and 0% of the reported population (0 people) lives in districts projected to cross a +0.5-phase-point increase, holding population at its current level. Under SSP585 by the 2050s, the population-weighted mean change in lean-season IPC phase is a rise of 0.094, and 2% of the reported population (349,703 people) lives in districts projected to cross a +0.5-phase-point increase, holding population at its current level. Projections cover 80 of the 84 units under SSP2-4.5 and 79 under SSP5-8.5 (Table 7 note). This is an illustration of direction and rough magnitude under the paper's own fitted relationship, not a probabilistic forecast (Section 6). Figure 13 maps the projected change by district and scenario; Figure S12 and Table 7 summarise the population-weighted burden.

This manuscript is a preprint and has not been peer reviewed. The copyright holder has made the manuscript available under a Creative Commons Attribution 4.0 International (CC BY) license and consented to have it forwarded to EarthArXiv for public posting.

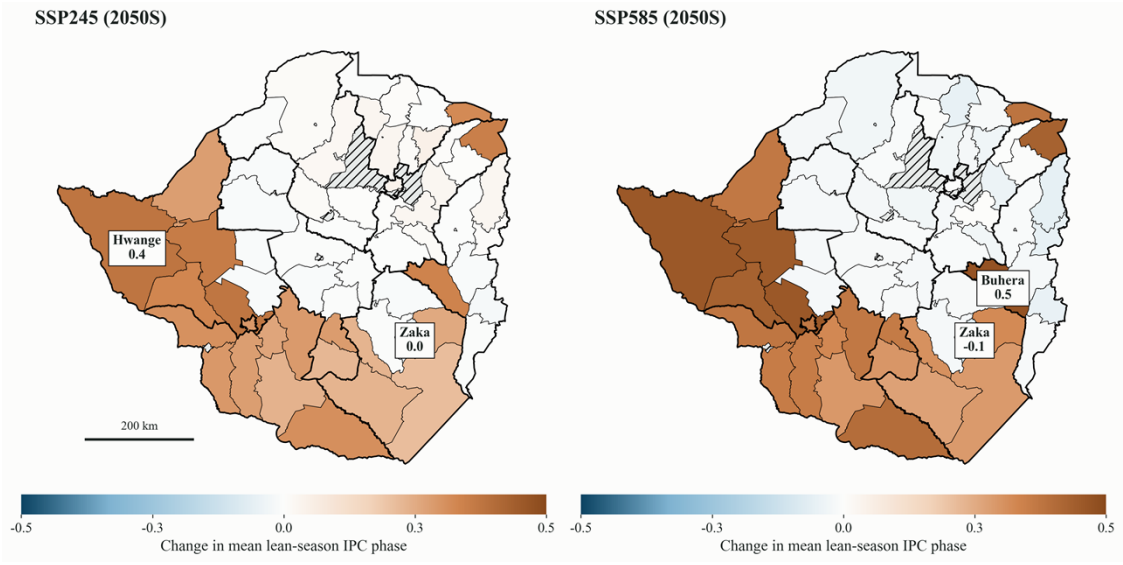


Figure 13. Projected change in mean lean-season IPC phase by district under each CMIP6 scenario, 2050s against the 1995-2014 historical reference, delta method (Section 3.8). Diverging scale: some districts may project cooler or wetter.

Table 7. Projected population-weighted phase change and elevated-risk population share under each climate scenario, 2050s.

scenario	total population	mean delta phase	mean delta phase population weighted	elevated risk threshold	elevated risk population	elevated risk share
ssp245_2050s	14,586,559	0.1107	0.0908	0.5000	0.0000	0.0000
ssp585_2050s	14,491,828	0.1246	0.0944	0.5000	349,703	0.0241

Note. Totals cover the units for which a projection could be computed: 80 of 84 under SSP2-4.5 and 79 under SSP5-8.5. Gokwe South Urban, Goromonzi, Ruwa and Zvimba drop out of both scenarios, and Kadoma Urban drops out of SSP5-8.5 only, because the projected hot-day count lies above the historical maximum and the two highest historical counts are tied, which leaves the linear extrapolation step undefined. The difference in total population between the scenarios (94,731) is the

This manuscript is a preprint and has not been peer reviewed. The copyright holder has made the manuscript available under a Creative Commons Attribution 4.0 International (CC BY) license and consented to have it forwarded to EarthArXiv for public posting.

population of Kadoma Urban; population is otherwise identical across scenarios and held at its current level.

5. Discussion

5.1 Principal findings

Pooled across Zimbabwe, the compound drought-heat interaction is small, only marginally significant under clustered inference, loses significance under the spatially robust Conley standard error, and does not improve leave-one-season-out prediction relative to simpler specifications: on the pooled evidence alone, this would read as a weak or null result. That reading is incomplete. The same interaction, estimated separately by agro-ecological stratum, is large and precisely estimated in the driest third of the country, and a pooled three-way interaction test, the specification that can actually adjudicate between strata rather than merely display them side by side, shows that this stratum differs from the wettest third (+0.051, $p = 0.029$), although the joint test across all three strata is weaker ($p = 0.087$). Unlike the pooled estimate, the driest-third estimate survives Conley errors at every cutoff and the season-block permutation ($p = 0.004$). The honest summary is not “the compound effect is real” or “the compound effect is absent”; it is that the compound mechanism operates where marginal land is farmed at all and is averaged away to near-invisibility by any specification that treats Zimbabwe as one unit.

Part of the pooled result is a power question, not only a magnitude question. At the pooled clustered standard error (0.0175), the design has 80 per cent power to detect an interaction of about 0.049 phase units at the 5 per cent level; the pooled point estimate itself (+0.030) falls below that threshold, so a marginal p-value there is close to what an underpowered test for an effect of this size would produce even if

This manuscript is a preprint and has not been peer reviewed. The copyright holder has made the manuscript available under a Creative Commons Attribution 4.0 International (CC BY) license and consented to have it forwarded to EarthArXiv for public posting.

the true pooled effect were exactly this small, not evidence that it is zero. The driest third estimate (+0.116, standard error 0.034) clears its own comparable threshold (about 0.095) comfortably, so that result is not an artefact of a subgroup that happened to be better powered by chance.

This resolves what would otherwise look like a contradiction between the national and the stratified results. A pooled estimator asks whether heat systematically amplifies drought's effect everywhere; the answer is no. A stratified estimator asks whether it does so anywhere; the answer is yes, and specifically in the Natural Region IV/V-type districts where communal-area households cultivate maize on land who's own agro-ecological classification says it should carry livestock, not a moisture-and-heat-sensitive cereal. The 2015/16 season, one of the worst El Niño droughts on record for the region, illustrates the exposure side of this at the national level even where it does not resolve the outcome side cleanly: 69 per cent of districts were classified jointly in drought and heat stress that season, the highest share anywhere in the panel and far above every other year, sitting inside a two-year window (2014 to 2016) in which the population-weighted national mean lean-season phase rose from 1.0 to just over 2.0. The single sharpest year-on-year rise in the whole 2009-2025 record in fact precedes the compound spike by one season (2014 to 2015, phase 1.0 to 1.93, when the binary compound share was still zero), a reminder that the national mean is a noisy, aggregate quantity and not itself evidence for or against the compound mechanism; the stratified estimate in Section 4.7 is.

This manuscript is a preprint and has not been peer reviewed. The copyright holder has made the manuscript available under a Creative Commons Attribution 4.0 International (CC BY) license and consented to have it forwarded to EarthArXiv for public posting.

5.2 Why pooling hides the effect

Two features of the data explain why a national average is the wrong scale to test this claim at. First, the districts where the mechanism is strongest are also, by construction of the aridity stratification, the driest third of the country, so their growing-season hot-day counts and their moisture deficits are less independent of each other there than elsewhere: heat and drought already move together on marginal land, which is exactly the joint-tail condition the compound-event framing is built to detect, and exactly the condition a rainfall-only or an additive specification cannot separate from ordinary drought severity. Second, the wetter two-thirds of the country supply most of the panel's statistical power, simply because that is where more districts and more stable food-security reporting sit, so a pooled coefficient is closer to a population-weighted average dominated by places where the mechanism is weak than to a test of whether the mechanism exists.

5.3 Implications for monitoring

Three consequences follow. First, a single national compound-risk indicator is not the right product: it will be approximately correct for most of the country and will miss the risk precisely where it is largest, in the same marginal districts that already carry the least buffering capacity against a bad season. Second, the stratified estimate, not the pooled one, is the operationally relevant number for the Natural Region IV/V districts specifically, and food security outlooks for those districts should weigh a compound drought-heat signal accordingly. Third, because the underlying data (ERA5-Land, CHIRPS) are already operational and the district-specific hot-day

This manuscript is a preprint and has not been peer reviewed. The copyright holder has made the manuscript available under a Creative Commons Attribution 4.0 International (CC BY) license and consented to have it forwarded to EarthArXiv for public posting.

threshold this paper uses are a per-stratum quantity by construction, stratifying the monitoring product is a reporting change, not a new observation system.

5.4 What the fixed effects can and cannot rule out

Within-district identification is strong protection against confounding by fixed characteristics, but it does not address time-varying district-level confounders that correlate with weather, most obviously conflict, market disruption and targeted food aid. Aid is a live concern: districts classified into higher phases receive assistance, which mechanically compresses the measured outcome and biases estimates toward zero nationally and more where aid delivery is easier, i.e. in the wetter, more accessible two-thirds of the country. If so, part of why the pooled effect is small is the same reason the stratified effect is not: the driest districts may be both where the physical mechanism is strongest and where compensating aid is least able to attenuate it. The estimates here are therefore best read as lower bounds on the uncompensated effect, and more so in the pooled specification than in the driest-tercile one.

6. Limitations

i. **The outcome is a classification, not a** measurement: IPC phases are produced by analyst consensus against evidence, not by direct observation of a continuous quantity. They are ordinal, coarse, and subject to changes in analytical convention over time. Aggregating three monthly classifications to a lean-season means mitigating but does not remove this.

ii. **Aid response:** As noted above, humanitarian assistance is triggered by the outcome, attenuating estimated effects. Quantifying this would require district-level assistance data that is not consistently available.

This manuscript is a preprint and has not been peer reviewed. The copyright holder has made the manuscript available under a Creative Commons Attribution 4.0 International (CC BY) license and consented to have it forwarded to EarthArXiv for public posting.

iii. **Rainfall product uncertainty**: Zimbabwe's gauge network has thinned since 2000, so CHIRPS skill is not constant over the study period. Section 4.9 re-estimates an independent product, but that product is reanalysis rather than gauge-calibrated, so it bounds sensitivity to product choice without resolving accuracy. A TAMSAT-based replication would be the stronger check.

iv. **Ecological inference**: Districts average 6,500 km² and span considerable internal agro-ecological variation. District-level associations do not license household-level claims.

v. **Modifiable areal unit problem:** Results are conditional on the FEWS NET district geometry. We do not test sensitivity to alternative aggregations, which would require the outcome at a different scale. Conley standard errors address spatial correlation in the errors but not the choice of areal unit itself.

vi. **Stratum assignment:** Where Natural Regions are used, districts spanning more than one region are assigned a modal region, which discards within-district agro-ecological variation. Where the aridity-tercile fallback is used, the strata are a rainfall proxy, and the heterogeneity results should not be read as statements about Natural Regions.

vii. **Exposure window**: We fix the growing season at October to March nationally. Planting dates vary across Natural Regions and between seasons, so a fixed window introduces measurement error that is larger in the marginal regions.

viii. **Scenario projection**: Section 4.10's projection extrapolates a relationship fitted on 2009-2025 to a 2046-2065 climate outside that record's range for some districts and carries forward the same measurement and confounding

This manuscript is a preprint and has not been peer reviewed. The copyright holder has made the manuscript available under a Creative Commons Attribution 4.0 International (CC BY) license and consented to have it forwarded to EarthArXiv for public posting.

limitations (aid response, above) rather than resolving them. It assumes the diurnal temperature range is unchanged under warming, holds population at current levels, and applies each district's fitted or stratum-level coefficients without a further correction for the fact that those coefficients were themselves estimated with uncertainty; the projection therefore does not carry its own confidence interval and should be read as an illustration of direction and rough magnitude under the paper's own fitted relationship, not as a probabilistic forecast. A single time horizon and a two-scenario SSP2-4.5/SSP5-8.5 comparison is a deliberate scope decision, not a technical limit of the method.

ix.

7. Conclusion

Moisture deficit and growing-season heat interact in their effect on lean-season food insecurity in Zimbabwe, but not everywhere: the effect is concentrated in the driest third, where communal-area maize cultivation already sits at the edge of what the land supports. A national average is the wrong scale to test this claim at; monitoring that pools all districts together will miss a real, localized risk that a stratified assessment recovers.

The pipeline is released in full and is parameterized in country. Replication elsewhere requires setting the country code, and for bimodal-rainfall countries, redefining the growing and lean seasons, which is a modelling decision rather than a configuration one. Given that compound drought-heat conditions are projected to become more frequent across the region, and that the marginal cost of adding a

This manuscript is a preprint and has not been peer reviewed. The copyright holder has made the manuscript available under a Creative Commons Attribution 4.0 International (CC BY) license and consented to have it forwarded to EarthArXiv for public posting.

temperature term to operational monitoring is close to zero, the case for testing this elsewhere is straightforward

.

Declarations

Funding.

This research received no specific grant from any funding agency.

Competing interests. None declared.

Ethics. This study uses only publicly available, de-identified, area-level administrative data (harmonized food security classifications and gridded climate products). No individual-level or personally identifiable data are used, and no ethics approval was required.

Credit authorship contribution statement. Handsome Bongani Nyoni: Conceptualization, Methodology, Formal analysis, Data curation, Visualization, Writing - original draft. Mashford Zenda conceptualization ,methodology ,Formal analysis .Happy Mathew Tirivangasi, Perez Livias Moyo , Lesly Chawira, Zororo Chinwadzimba and Rutendo Sibanda writing - review & editing, Validation.

Data availability. This study used only publicly available data; no new primary data were collected. The harmonised food-insecurity classifications and FEWS NET administrative boundaries used in this study are available from the World Bank Data Catalog, "Harmonized Sub-National Food Security Data" (entry 0064614), under a CC BY 4.0 license, at https://datacatalog.worldbank.org/search/dataset/0064614 . CHIRPS version 3 precipitation data were accessed via Google Earth Engine at https://developers.google.com/earth-engine/datasets/catalog/UCSB-CHC_-

This manuscript is a preprint and has not been peer reviewed. The copyright holder has made the manuscript available under a Creative Commons Attribution 4.0 International (CC BY) license and consented to have it forwarded to EarthArXiv for public posting.

CHIRPS_V3_DAILY-_RNL. ERA5-Land climate reanalysis data were accessed via Google Earth Engine at https://developers.google.com/earth-engine/-datasets/catalog/ECMWF_ERA5_LAND_DAILY_AGGR. The analysis pipeline and Earth Engine extraction scripts are available at Zenodo, https://doi.org/10.5281/zenodo.23538495.

References

AghaKouchak, A., Chiang, F., Huning, L. S., Love, C. A., Mallakpour, I., Mazdiyasni, O., Moftakhari, H., Papalexiou, S. M., Ragno, E., & Sadegh, M. (2020). Climate extremes and compound hazards in a warming world. *Annual Review of Earth and Planetary Sciences*, *48*(1), 519-548. https://doi.org/10.1146/annurev-earth-071719-055228

Cohen, I., Zandalinas, S. I., Huck, C., Fritschi, F. B., & Mittler, R. (2021). Meta-analysis of drought and heat stress combination impact on crop yield and yield components. *Physiologia Plantarum*, *171*(1), 66-76. https://doi.org/10.1111/ppl.13203

Funk, C., Peterson, P., Harrison, L., Saldivar, R., Landsfeld, M., Pedreros, D., Shukla, S., Fink, A. H., Davenport, F., Peterson, S., Turner, W., Sonnier, A., Budde, M., Tabor, K., Verdin, J., Hauzaree, D., Naim, M., Alaso, D., & Husak, G. (2026). The Climate Hazards Center Infrared Precipitation with Stations, Version 3. *Scientific Data*, *13*(1), 718. https://doi.org/10.1038/s41597-026-07096-4

Funk, C., Peterson, P., Landsfeld, M., Pedreros, D., Verdin, J., Shukla, S., Husak, G., Rowland, J., Harrison, L., Hoell, A., & Michaelsen, J. (2015). The climate hazards infrared precipitation with stations: A new environmental record for

This manuscript is a preprint and has not been peer reviewed. The copyright holder has made the manuscript available under a Creative Commons Attribution 4.0 International (CC BY) license and consented to have it forwarded to EarthArXiv for public posting.

monitoring extremes. *Scientific Data*, *2*(1), 150066. https://doi.org/10.1038/sdata.2015.66

Hargreaves, G. H., & Samani, Z. A. (1985). Reference crop evapotranspiration from temperature. *Applied Engineering in Agriculture*, *1*(2), 96-99. https://doi.org/10.13031/2013.26773

Machefer, M., Ronco, M., Thomas, A.-C., Assouline, M., Rabier, M., Corbane, C., & Rembold, F. (2025). A monthly sub-national Harmonized Food Insecurity Dataset for comprehensive analysis and predictive modeling. *Scientific Data*, *12*(1), 741. https://doi.org/10.1038/s41597-025-05034-4

Maidment, R. I., Quaife, T., Pinnington, E., Black, E., Ejigu, A., Kumar, D., & Thomas, S. (2026). A new, long-term root zone soil moisture dataset for operational agricultural drought monitoring over Africa. *Scientific Data*, *13*(1), 260. https://doi.org/10.1038/s41597-026-06585-w

Manatsa, D., Mushore, T., & Lenouo, A. (2017). Improved predictability of droughts over southern Africa using the standardized precipitation evapotranspiration index and ENSO. *Theoretical and Applied Climatology*, *127*(1-2), 259-274. https://doi.org/10.1007/s00704-015-1632-6

McKee, T. B., Doesken, N. J., & Kleist, J. (1993). The relationship of drought frequency and duration to time scales. *Proceedings of the 8th Conference on Applied Climatology*, 179-184.

Muñoz-Sabater, J., Dutra, E., Agustí-Panareda, A., Albergel, C., Arduini, G., Balsamo, G., Boussetta, S., Choulga, M., Harrigan, S., Hersbach, H., Martens, B., Miralles, D. G., Piles, M., Rodríguez-Fernández, N. J., Zsoter, E.,

This manuscript is a preprint and has not been peer reviewed. The copyright holder has made the manuscript available under a Creative Commons Attribution 4.0 International (CC BY) license and consented to have it forwarded to EarthArXiv for public posting.

Buontempo, C., & Thépaut, J.-N. (2021). ERA5-Land: A state-of-the-art global reanalysis dataset for land applications. *Earth System Science Data*, *13*(9), 4349-4383. https://doi.org/10.5194/essd-13-4349-2021

Peng, J., Dadson, S., Hirpa, F., Dyer, E., Lees, T., Miralles, D. G., Vicente-Serrano, S. M., & Funk, C. (2020). A pan-African high-resolution drought index dataset. *Earth System Science Data*, *12*(1), 753-769. https://doi.org/10.5194/essd-12-753-2020

Rudolph, M., & Zenda, M. (2025). The social, economic and environmental impact of an agroecological farming system: A case study in Phumulani Agri-village, Belfast, Mpumalanga, South Africa. Frontiers in Sustainable Food Systems, 9, 1519382. https://doi.org/10.3389/fsufs.2025.1519382

Schlenker, W., & Lobell, D. B. (2010). Robust negative impacts of climate change on African agriculture. *Environmental Research Letters*, *5*(1), 014010. https://doi.org/10.1088/1748-9326/5/1/014010

Vicente-Serrano, S. M., Beguería, S., & López-Moreno, J. I. (2010). A multiscalar drought index sensitive to global warming: The standardized precipitation evapotranspiration index. *Journal of Climate*, *23*(7), 1696-1718. https://doi.org/10.1175/2009JCLI2909.1

Zenda, M. (2024). A systematic literature review on the impact of climate change on the livelihoods of smallholder farmers in South Africa. *Heliyon*, *10*(18), e38162. https://doi.org/10.1016/j.heliyon.2024.e38162

This manuscript is a preprint and has not been peer reviewed. The copyright holder has made the manuscript available under a Creative Commons Attribution 4.0 International (CC BY) license and consented to have it forwarded to EarthArXiv for public posting.

794 Zenda, M. (2026). Climate change and food security in sustainable finance: A South
795 African perspective. *Frontiers in Climate*, *8*, 1926592.
796 https://doi.org/10.3389/fclim.2026.1926592

797 Zenda, M., Tirivangasi, H. M., & Mazenda, A. (2026). The role of climate-smart
798 agriculture in strengthening South Africa's food system and climate response.
799 Management of Environmental Quality: An International Journal, 1-24.

800 Zimbabwe Livelihoods Assessment Committee. (2025). *2025 Rural Livelihoods*
801 *Assessment Report*. Food and Nutrition Council.

802
803 Zscheischler, J., Martius, O., Westra, S., Bevacqua, E., Raymond, C., Horton, R. M.,
804 van den Hurk, B., AghaKouchak, A., Jézéquel, A., Mahecha, M. D., Maraun, D.,
805 Ramos, A. M., Ridder, N. N., Thiery, W., & Vignotto, E. (2020). A typology of
806 compound weather and climate events. *Nature Reviews Earth & Environment*,
807 *1*(7), 333-347. https://doi.org/10.1038/s43017-020-0060-z

808 Zscheischler, J., Westra, S., van den Hurk, B. J. J. M., Seneviratne, S. I., Ward, P.
809 J., Pitman, A., AghaKouchak, A., Bresch, D. N., Leonard, M., Wahl, T., &
810 Zhang, X. (2018). Future climate risk from compound events. *Nature Climate*
811 *Change*, *8*(6), 469-477. https://doi.org/10.1038/s41558-018-0156-3

812
813

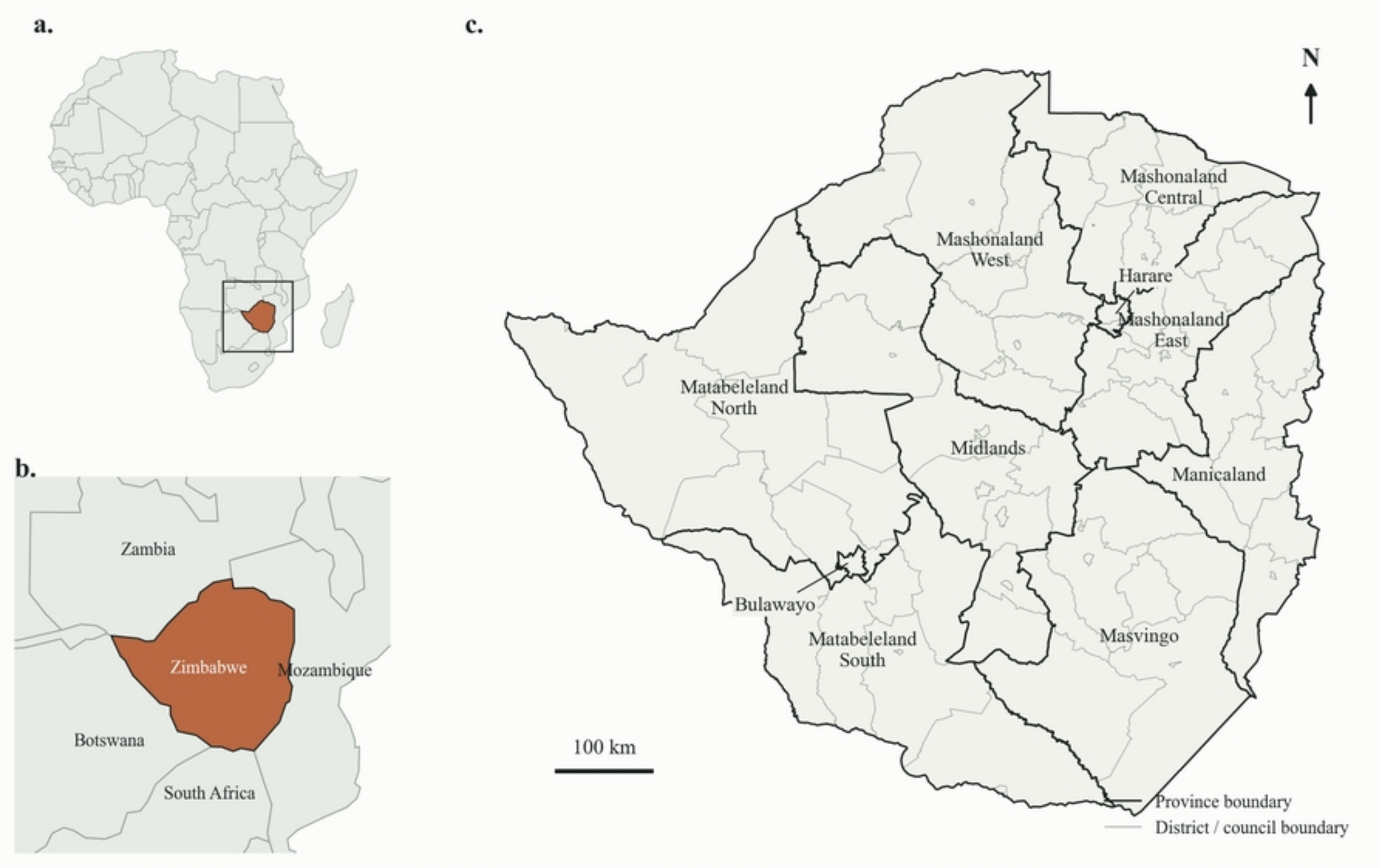

a.
b.
Zambia
Zimbabwe
Mozambique
Botswana
South Africa
c.
N
Mashonaland Central
Mashonaland West
Harare
Mashonaland East
Matabeleland North
Midlands
Manicaland
Bulawayo
Matabeleland South
Masvingo
100 km
Province boundary
District / council boundary

Figure 1

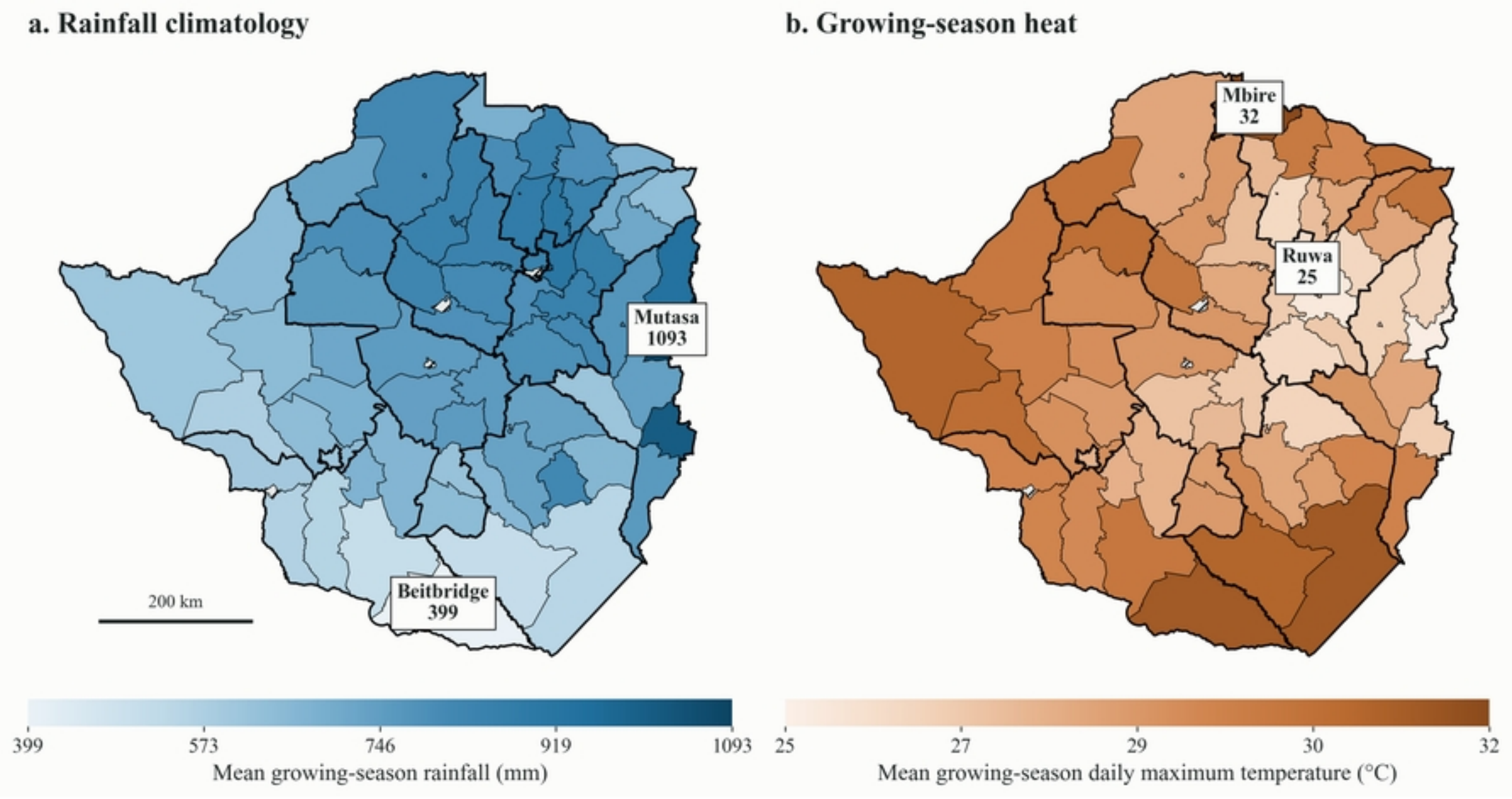

a. Rainfall climatology
Mutasa
1093
Beitbridge
399
200 km
399
573
746
919
1093
Mean growing-season rainfall (mm)
b. Growing-season heat
Mbire
32
Ruwa
25
25
27
29
30
32
Mean growing-season daily maximum temperature (°C)

Figure 2

This manuscript is a preprint and has not been peer reviewed. The copyright holder has made the manuscript available under a Creative Commons Attribution 4.0 International (CC BY) license and consented to have it forwarded to EarthArXiv for public posting.

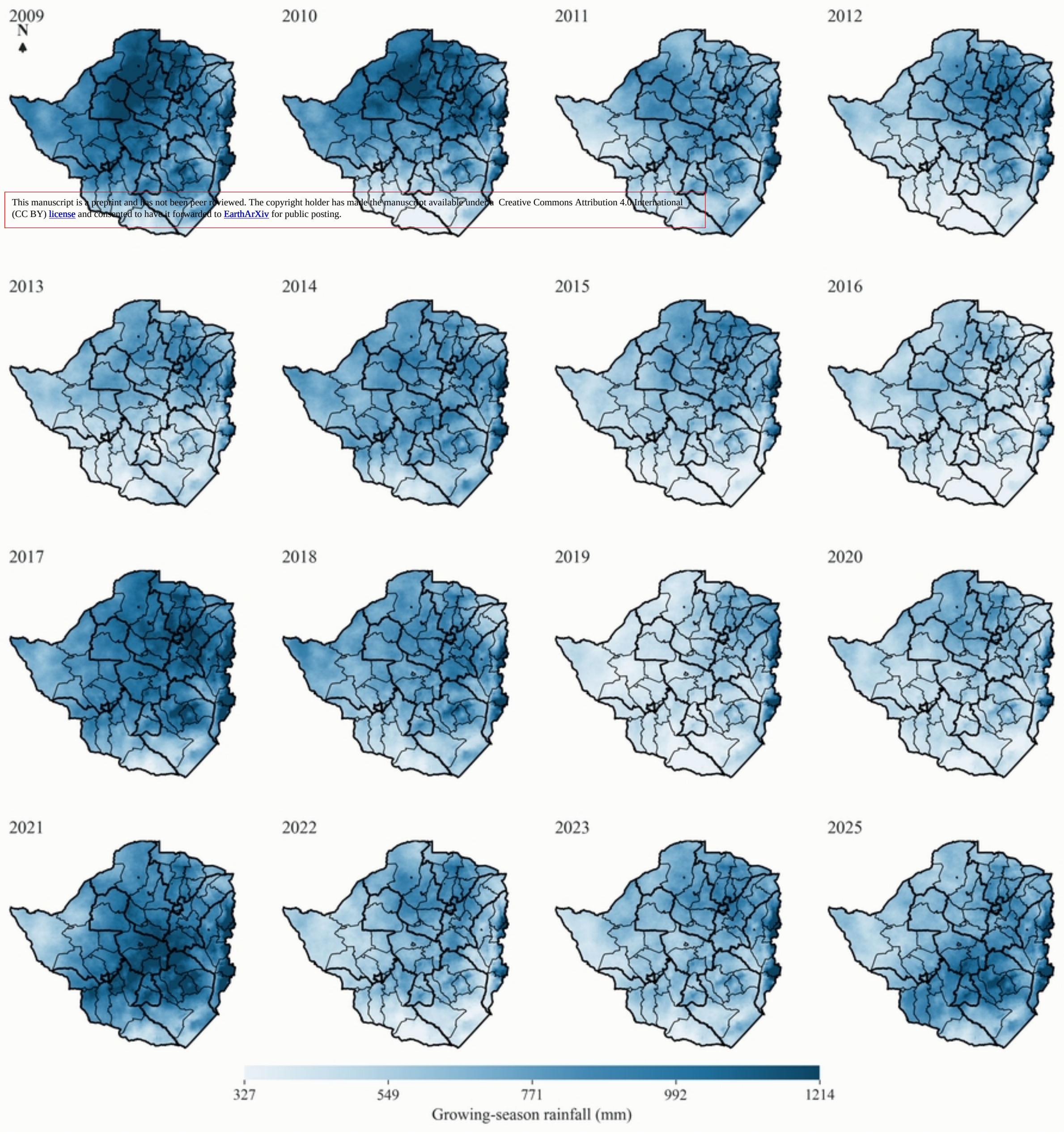


Figure 4

This manuscript is a preprint and has not been peer reviewed. The copyright holder has made the manuscript available under a Creative Commons Attribution 4.0 International (CC BY) license and consented to have it forwarded to EarthArXiv for public posting.

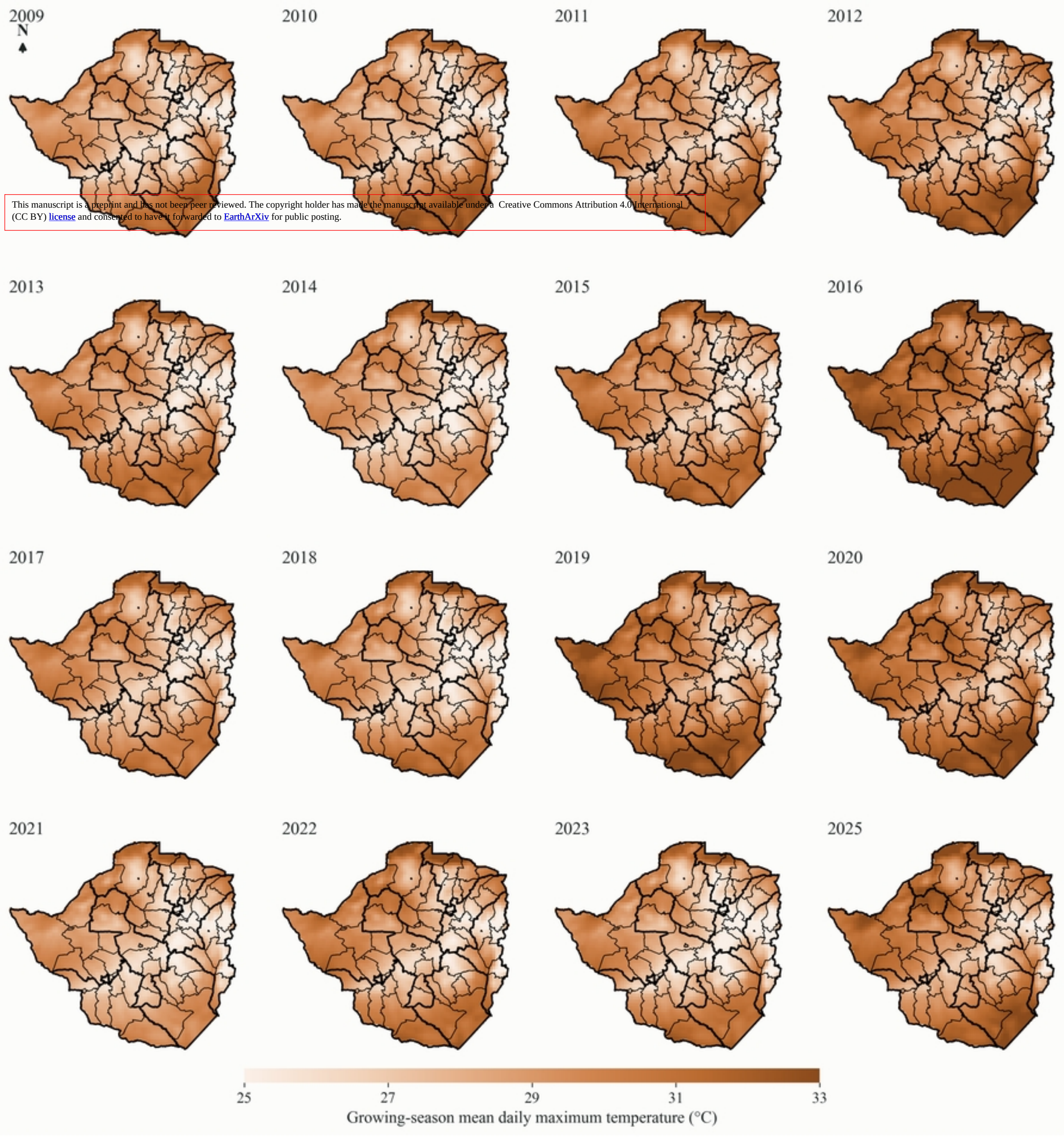


Figure 5

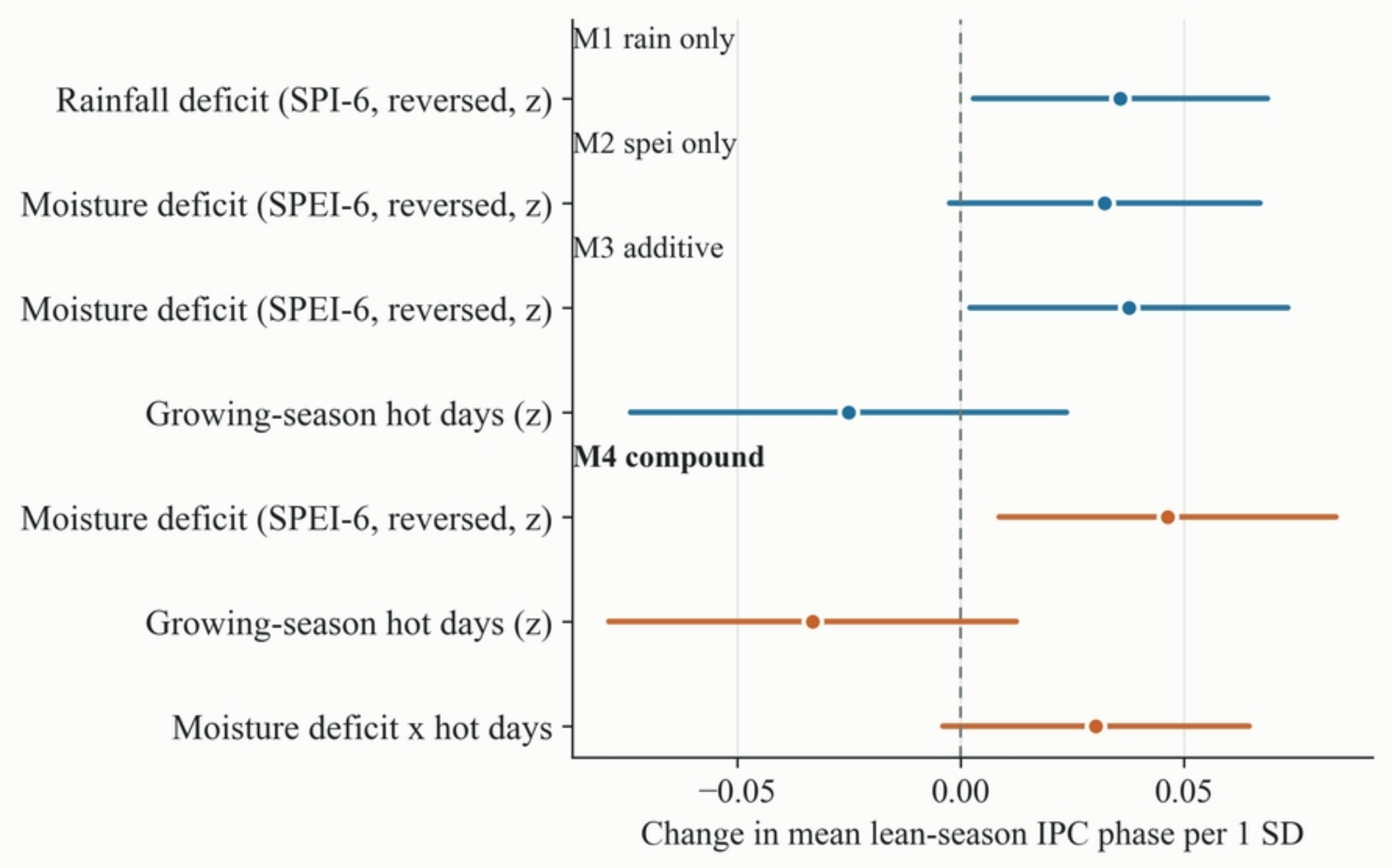

M1 rain only
Rainfall deficit (SPI-6, reversed, z)
M2 spei only
Moisture deficit (SPEI-6, reversed, z)
M3 additive
Moisture deficit (SPEI-6, reversed, z)
Growing-season hot days (z)
M4 compound
Moisture deficit (SPEI-6, reversed, z)
Growing-season hot days (z)
Moisture deficit x hot days
−0.05
0.00
0.05
Change in mean lean-season IPC phase per 1 SD

Figure 6

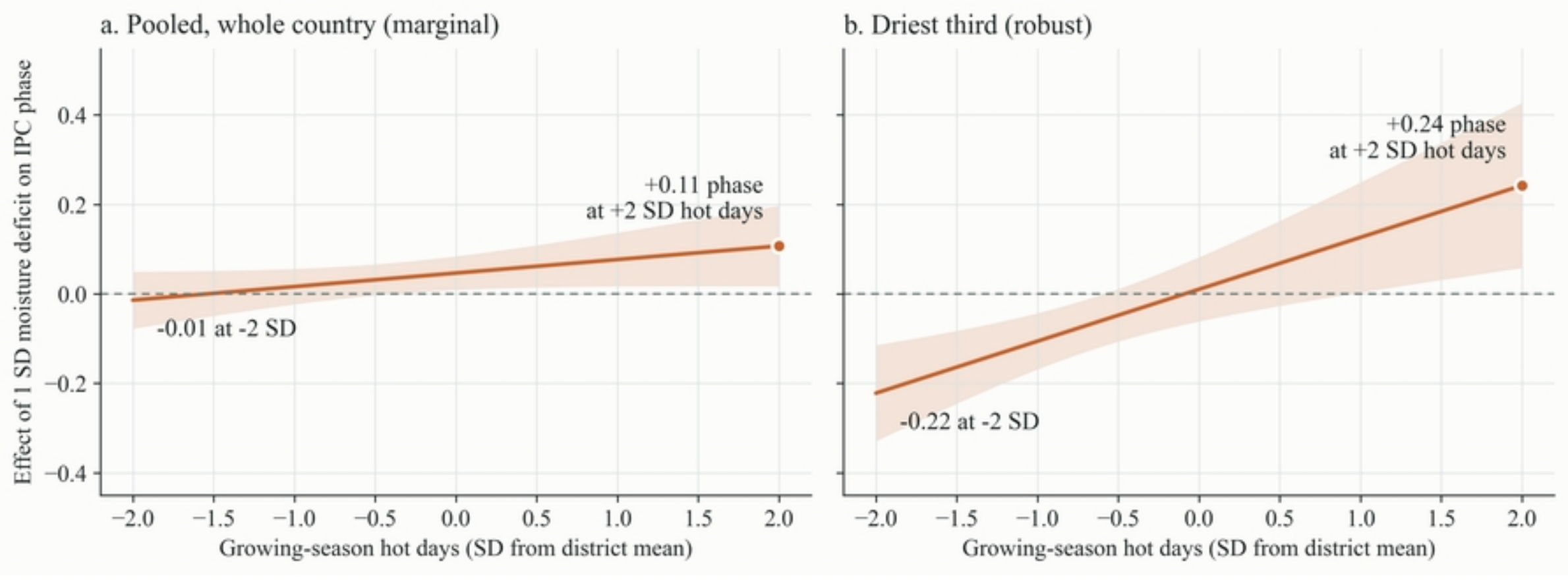

a. Pooled, whole country (marginal)
b. Driest third (robust)
Effect of 1 SD moisture deficit on IPC phase
0.4
0.2
0.0
−0.2
−0.4
+0.11 phase
at +2 SD hot days
-0.01 at -2 SD
+0.24 phase
at +2 SD hot days
-0.22 at -2 SD
−2.0
−1.5
−1.0
−0.5
0.0
0.5
1.0
1.5
2.0
Growing-season hot days (SD from district mean)
Growing-season hot days (SD from district mean)

Figure 7

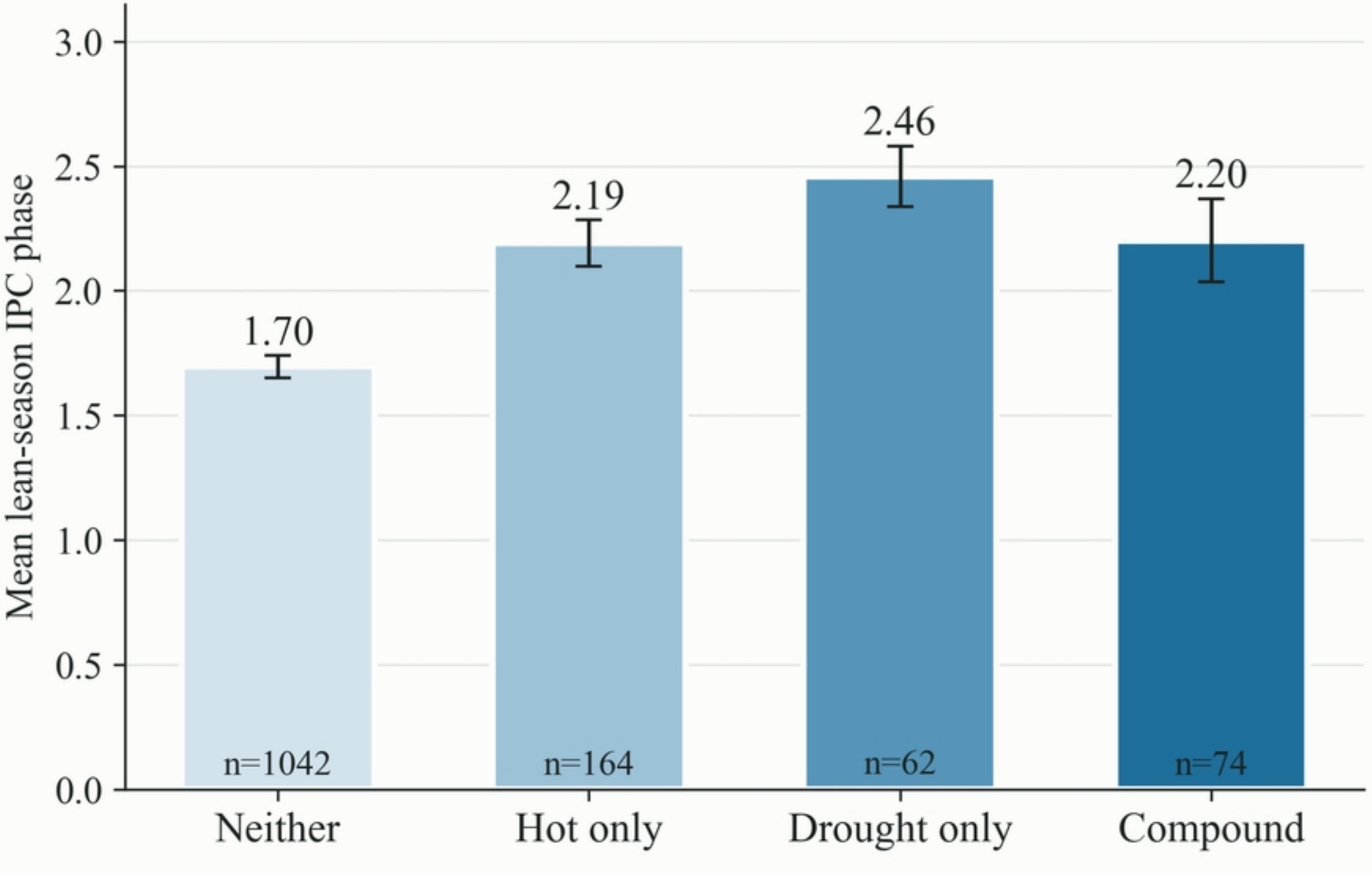

Mean lean-season IPC phase
3.0
2.5
2.0
1.5
1.0
0.5
0.0
1.70
2.19
2.46
2.20
n=1042
n=164
n=62
n=74
Neither
Hot only
Drought only
Compound

Figure 8

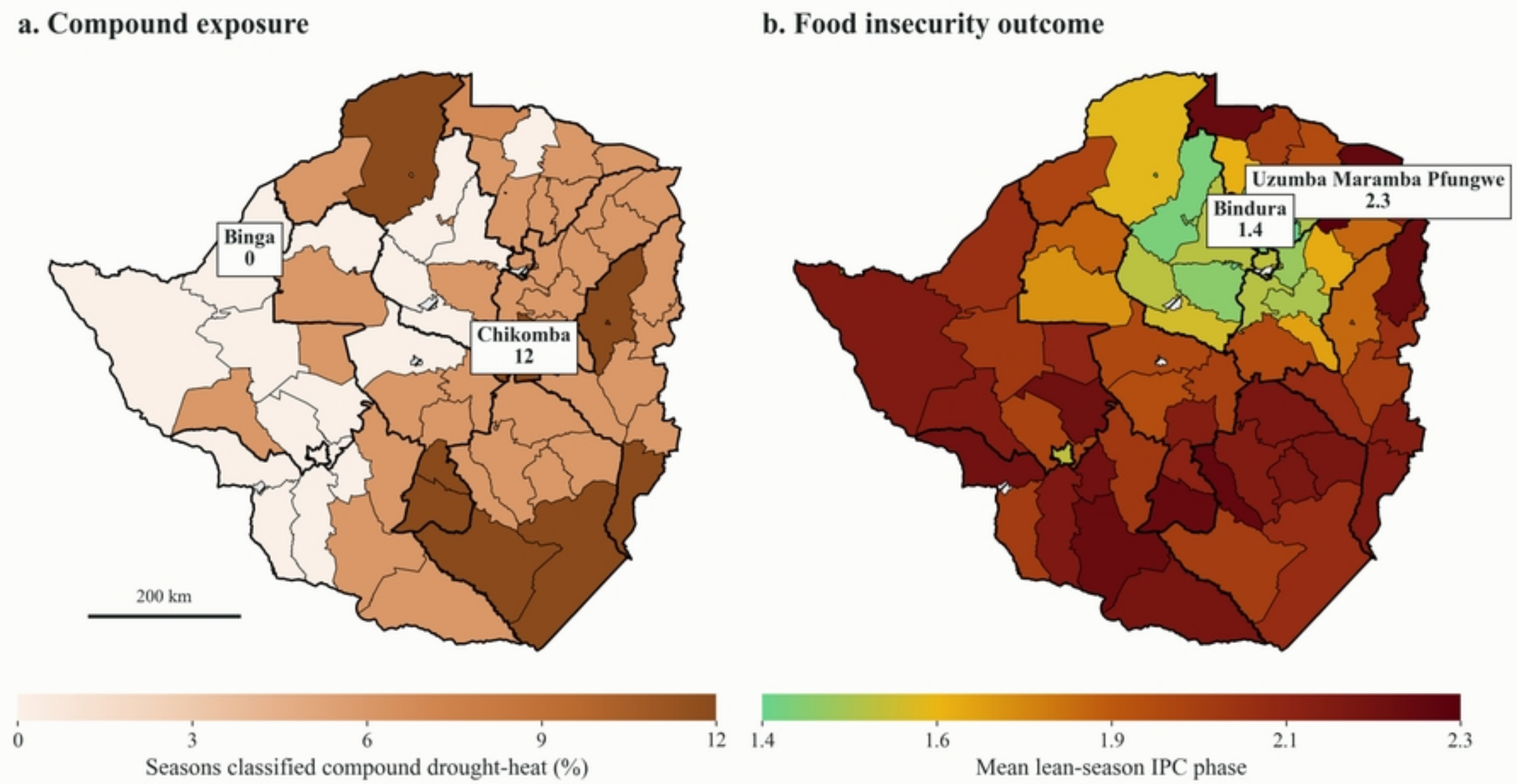

a. Compound exposure
b. Food insecurity outcome
Binga
0
Chikomba
12
200 km
Uzumba Maramba Pfungwe
2.3
Bindura
1.4
0
3
6
9
12
Seasons classified compound drought-heat (%)
1.4
1.6
1.9
2.1
2.3
Mean lean-season IPC phase

Figure 9

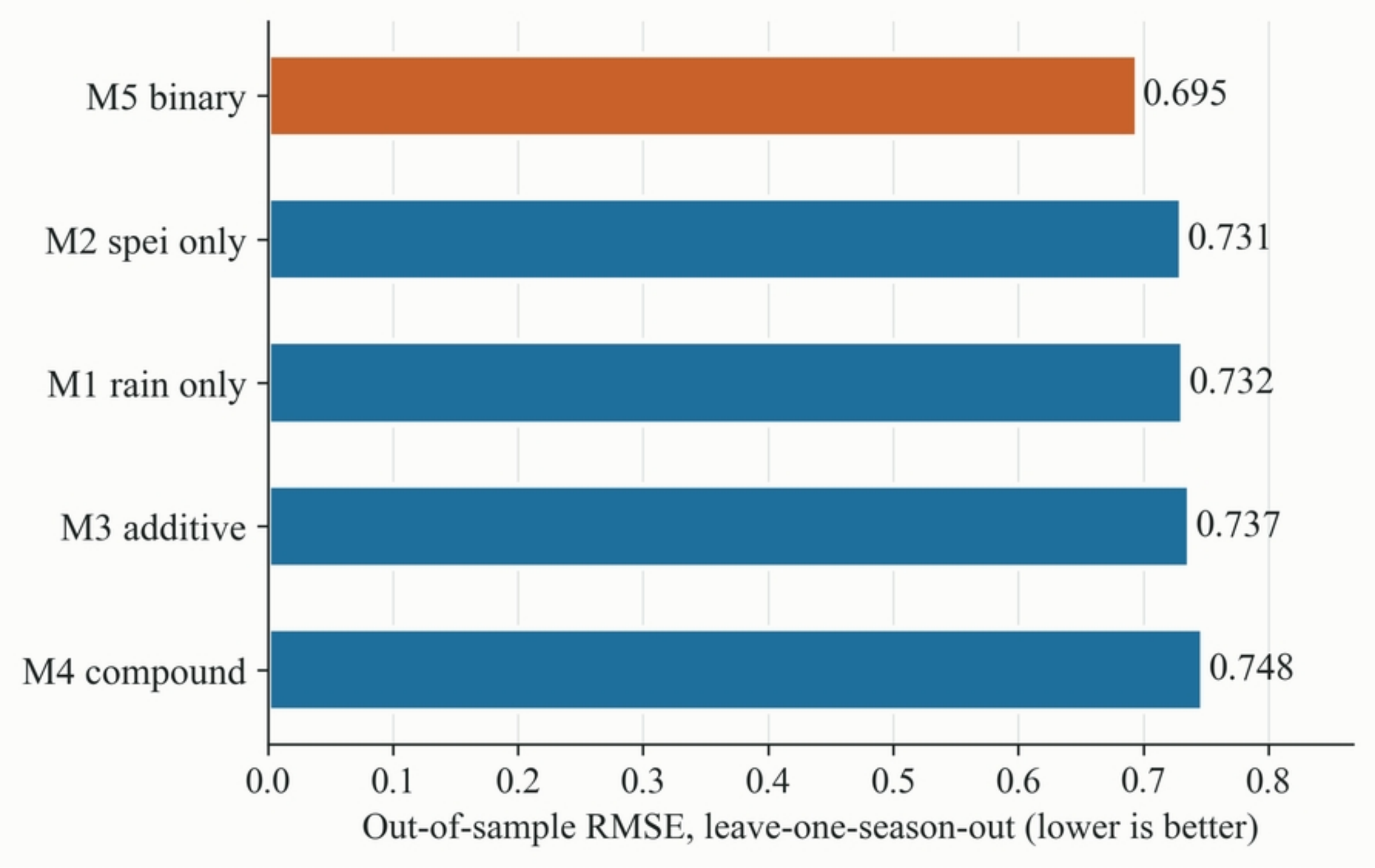

M5 binary
M2 spei only
M1 rain only
M3 additive
M4 compound
0.695
0.731
0.732
0.737
0.748
0.0
0.1
0.2
0.3
0.4
0.5
0.6
0.7
0.8
Out-of-sample RMSE, leave-one-season-out (lower is better)

Figure 10

This manuscript is a preprint and has not been peer reviewed. The copyright holder has made the manuscript available under a Creative Commons Attribution 4.0 International (CC BY) license and consented to have it forwarded to EarthArXiv for public posting.

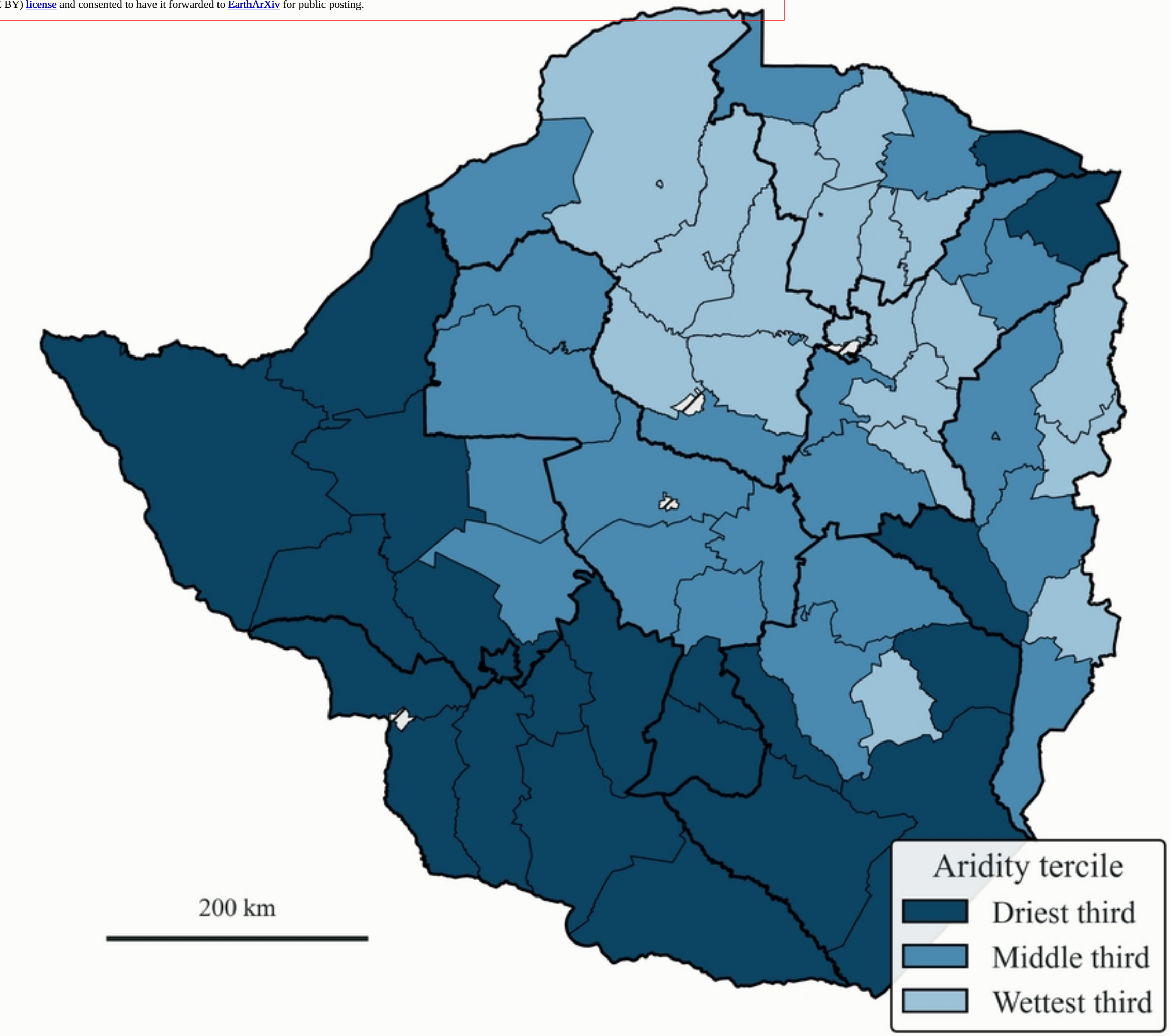


Figure 11

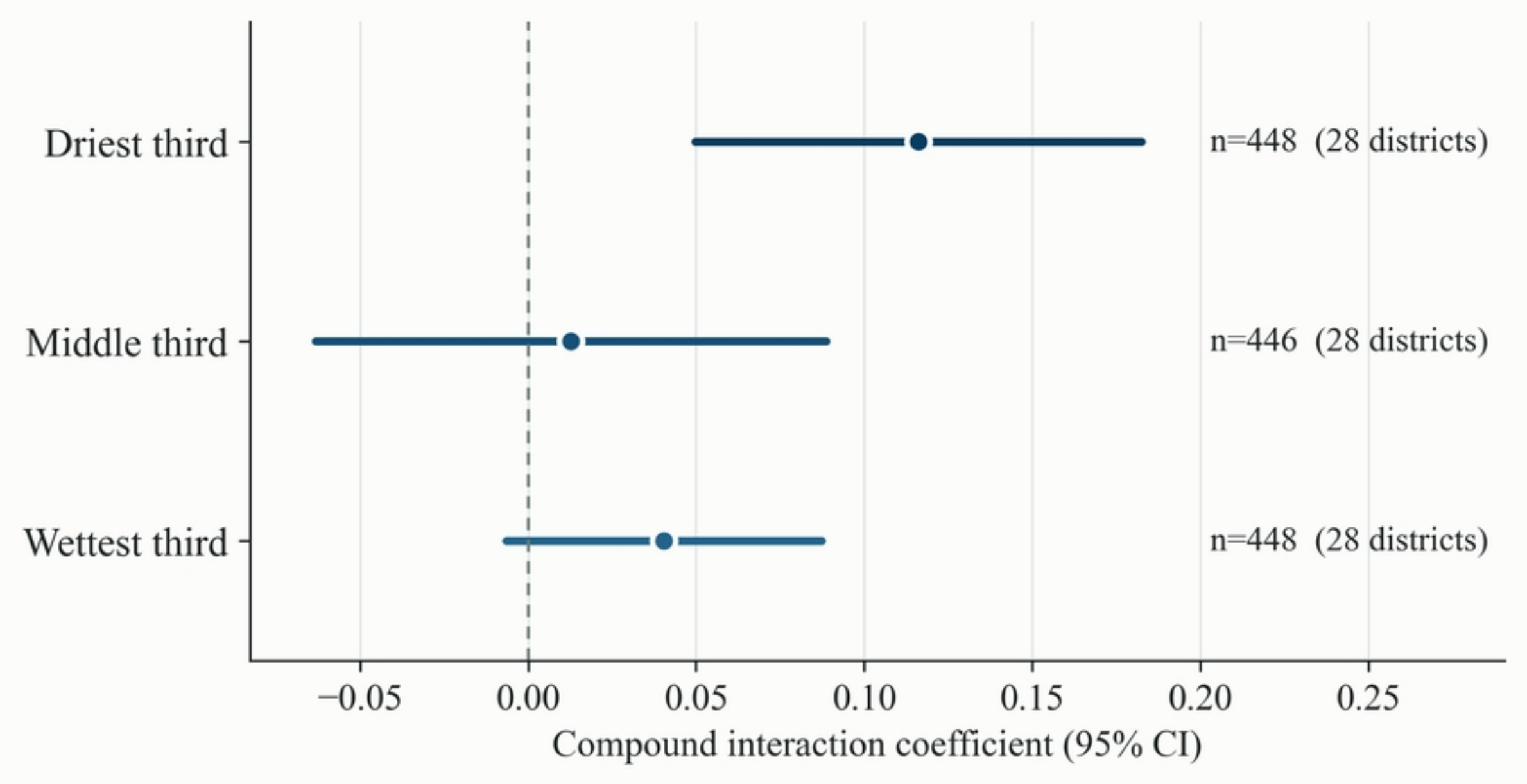

Driest third
Middle third
Wettest third
n=448 (28 districts)
n=446 (28 districts)
n=448 (28 districts)
−0.05
0.00
0.05
0.10
0.15
0.20
0.25
Compound interaction coefficient (95% CI)

Figure 12

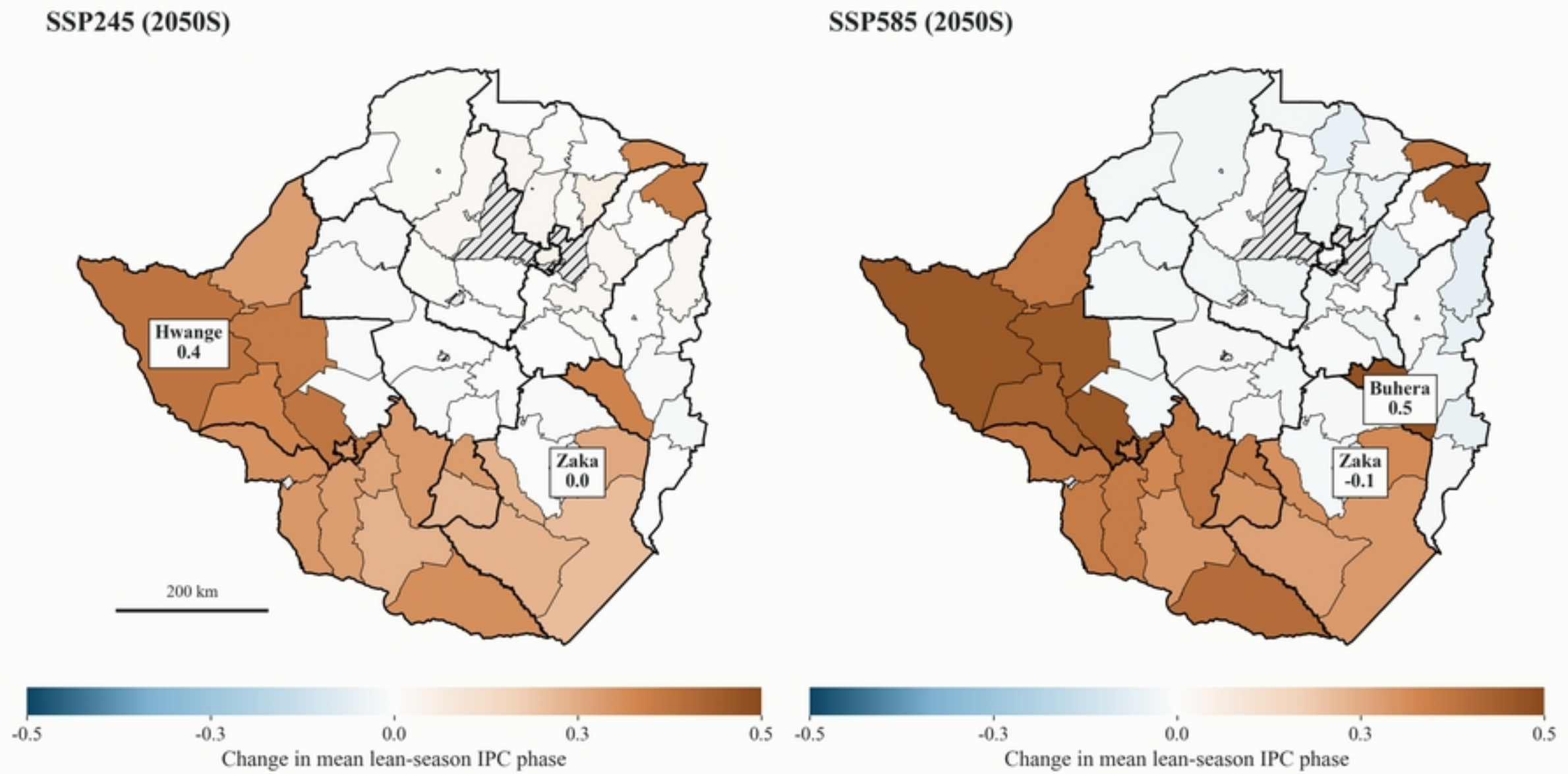

SSP245 (2050S)
Hwange
0.4
Zaka
0.0
200 km
-0.5
-0.3
0.0
0.3
0.5
Change in mean lean-season IPC phase
SSP585 (2050S)
Buhera
0.5
Zaka
-0.1
-0.5
-0.3
0.0
0.3
0.5
Change in mean lean-season IPC phase

Figure 13

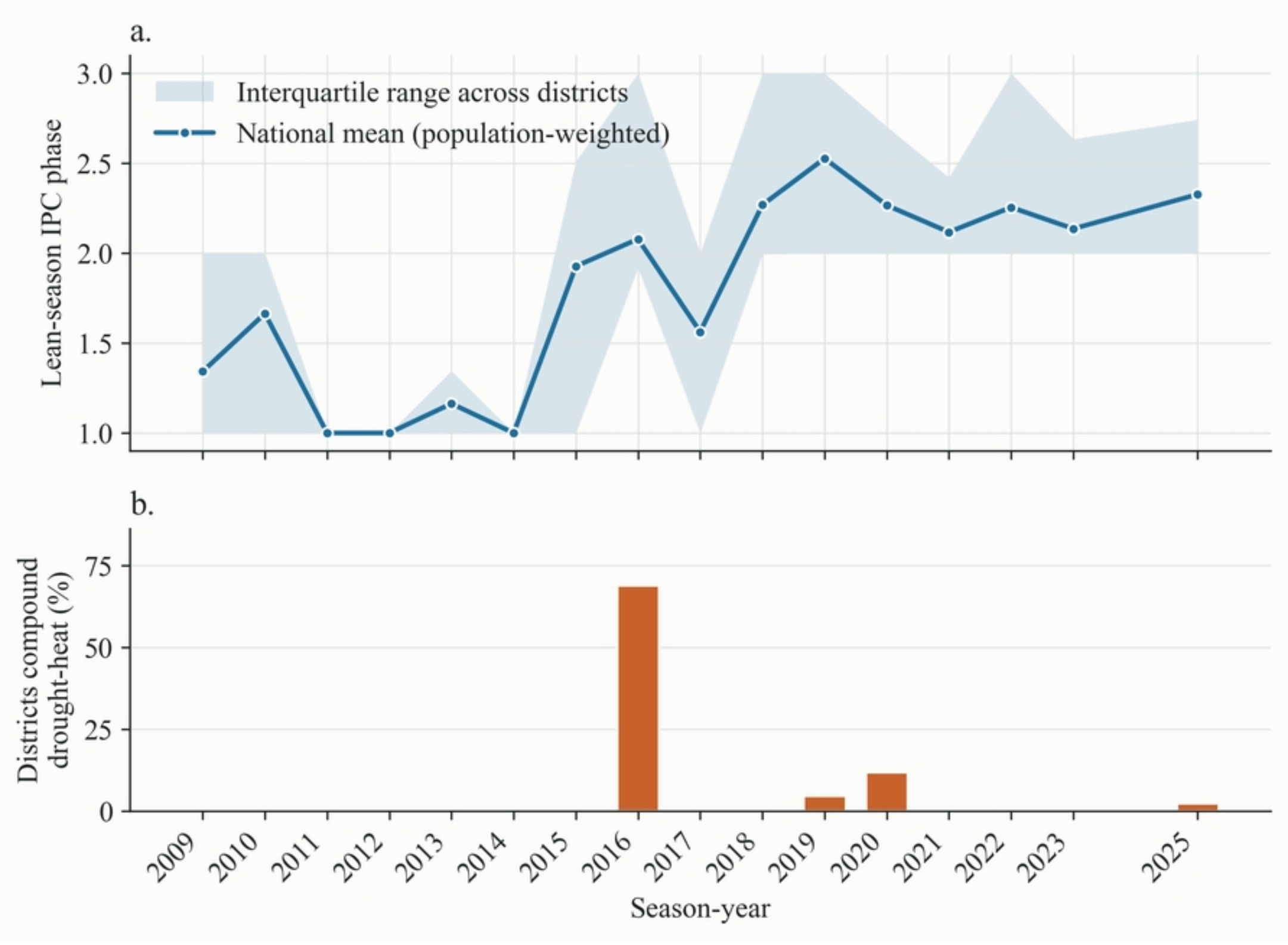

a.
Interquartile range across districts
National mean (population-weighted)
Lean-season IPC phase
3.0
2.5
2.0
1.5
1.0
b.
Districts compound drought-heat (%)
75
50
25
0
2009
2010
2011
2012
2013
2014
2015
2016
2017
2018
2019
2020
2021
2022
2023
2025
Season-year

Figure 3